The Academy of Prosthetic Dentistry R.O.C., Taiwan

Journal of Prosthodontics and Implantology

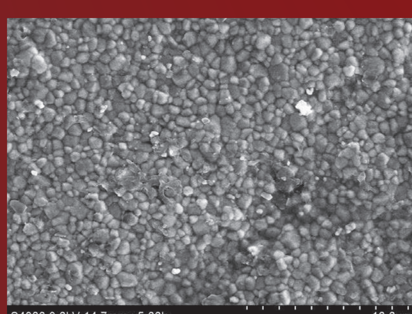

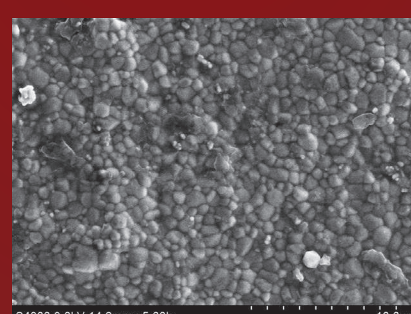

Effect of a Commercial Fluorescence Liquid on 3Y-TZP Surface Microstructure: A Preliminary Study. Page 16 Fig. 6 and Fig. 7

Official Journal of The Academy of Prosthetic Dentistry, R.O.C., Taiwan

Volume 7 Number 1
April 2018

Journal of Prosthodontics and Implantology

中華民國贋復牙科學會期刊

Vol.7, No.1
April 2018

Subscription：NT $2000/year　**訂價年費**：NT $2000（四期）
創刊日期：2012年4月
出版者：中華民國贋復牙科學會　**學會地址**：105台北市復興北路465號2樓　**學會電話**：(02)2546-8834
學會傳真：(02)2546-9157　**學會官網**：http://www.prosthod.org.tw
ISSN 2304-5418
承製編印：青田設計工作室　**地址**：235新北市中和區民富街64巷5-1號　**電話**：(02)2225-4014
E-mail：field.design@msa.hinet.net　**傳真**：(02)3234-5491

TABLE OF CONTENTS

Editorial

CAD-CAM, is it the only one way in the future?

200 years ago, people could not image how a vehicle can be moved from one place to another without horses to carriage it. After the invention of the aircraft, people not only can enjoy flying over the sea from one continental to the other, but also take the advantage of fast speed for time saving by the aircraft. Whenever we get one advantage, we always loss another at the same time. This is an ordinary regulation in the real world condition. If we take the advantage of speed to transfer from one continental to the other by an aircraft, we'll loss the capacity to carry hundreds of cargo by using a ship.

Thanks to the development of modern computer and material science, prosthetic dentistry has been turned into a brand new page. Limited abstracts regarding to the impression material like polysulfide, PVC have been presented in the IADR meeting, while more abstracts related to the precision of digital dentistry have been presented in different conferences. Computer aided design, computer aided manufacture (CAD-CAM) prosthetic dentistry in terms of digital dentistry becomes the major subject in many continue education courses.

There is one question raised, can CAD-CAM take the place of the traditional impression and manufacture process in prosthetic dentistry?

There is a beautiful island named Bali. Sun rising can be seen at every corner of the world. But if you want to enjoy the world well known rising sun at the top of the mountain in Bali island named Gunung Agung, horse riding is the only way to reach the top of the mountain for rising sun viewing. There is no doubt that computer science in terms of digital dentistry in the field of prosthetic dentistry will be the future trend in this field, but many procedures with highly technique sensitivity like color staining, esthetic design, can be reached only by dentist's mind and hand. Thus CAD-CAM can be a way lead to less time consuming, cost down the price but can not be aimed to take over all the traditional prosthetic dentistry that have been presented.

Let's enjoy the modern and traditional technique knowledge from this issue.

Allen Ming-Lun Hsu
Editor-in-Chief

Original Article

The Effect of Different Core/Veneer Thickness Ratios on Stress Distribution of Implant-supported Zirconia-ceramic Posterior Crowns: A 3-D Finite Element Analysis

Hui-Ling Chen, DDS, MS
Department of Dentistry National Yang-Ming University, Taipei, Taiwan

Chih-Ling Chang, DDS, MS, PhD
Assistant Professor, School of Dentistry National Yang-Ming University, Taipei, Taiwan
Director and Chief, Dental Department Shin Kong Wu Ho-Su Memorial Hospital, Taipei, Taiwan

Chen-Sheng Chen, DDS, MS, PhD
Department of Physical Therapy and Assistive Technology, National Yang-Ming University, Taipei, Taiwan

Ling-Ming Yu, DDS
Attending doctor, Department of Dentistry, Chang-Gung Memorial Hospital, Taipei, Taiwan

Ming-Lun Hsu, DDS, MS, PhD
Dean, School of Dentistry National Yang-Ming University, Taipei, Taiwan

Corresponding author:
Ming-Lun Hsu, DDS, MS, PhD
National Yang-Ming University
No.155, Linong St., Beitou Dist.,
Taipei City 11221, Taiwan R.O.C.
Tel: +886-2-2821-2943
E-mail: mlhsu@ym.edu.tw

Abstract

Purpose

To evaluate the effect of different core/veneer thickness ratios on stress distribution in implant-supported zirconia-ceramic posterior crowns.

Material and methods

Nonlinear contact finite element analysis was used to evaluate the stress distribution in zirconia-ceramic crowns under axial and oblique loading. Implant-supported maxillary first molar crowns with an occlusal thickness of 3 mm were constructed. Five models with the following different core/veneer thickness ratios were used: model I – 1/5 (0.5 mm/ 2.5 mm), model II – 1/2 (1 mm/ 2 mm), model III – 1/1 (1.5 mm/ 1.5 mm), model IV – 2/1 (2 mm/ 1 mm), and model V – 5/1 (2.5 mm/ 0.5 mm). The 1st principal stress and von Mises stress were analyzed to observe the effect of different core/veneer thickness ratios on the stress distribution.

Results

Whether under axial loading or oblique loading, the different core/veneer thickness ratios only affected the stress distribution in the core and veneer layer. The 1st principal stress results showed that the stress dissipation decreased as the core/veneer thickness ratio increased. The stress generated by oblique loading was greater than that generated by axial loading. Under axial loading, model V showed a higher maximum von Mises stress magnitude, but other models had no significant difference. As for oblique loading, model V also showed a higher maximum von Mises stress magnitude. Furthermore, model III and model IV revealed relatively favorable stress magnitudes in comparison with the other models.

Conclusion

The different core/veneer thickness ratios of the zirconia-ceramic crowns influenced the stress distribution on the crowns but not the implant component or supporting bone structures. Under axial loading, the core/veneer thickness ratio of 5/1 was unfavorable in terms of stress distribution. Meanwhile, the core/veneer thickness ratios of 1/5, 1/2, 1/1, and 2/1 showed no obvious differences with one another. As for oblique loading, the core/veneer thickness ratios of 1/1 and 2/1 were relatively favorable for stress distribution.

Keywards: core/veneer thickness ratio, finite element analysis, zirconia-ceramic restorations

Introduction

The current trend in prosthetic dentistry leads to metal-free restorations. The advances in CAD (computer-aided design)/CAM (computer-aided manufacturing) technology have enabled the frequent use of these high strength ceramic restorations in dentistry, especially those containing zirconia[1]. Zirconia had been used to make posts and cores, orthodontic brackets, frameworks for all-ceramic restorations, implant fixtures, and implant abutments[2]. As the core material for all-ceramic restorations, the opacity restrained the esthetic outcome compared to other all-ceramic systems. Therefore, the application of veneer porcelain over a zirconia core is often necessary to improve the esthetics of restoration containing zirconia. Such zirconia-ceramic restorations have become increasingly popular in the last few decades.

According to a literature review of the relevant clinical studies, the survival rates of zirconia-ceramic restorations consisting of either single crowns or fixed dental prostheses seem to be comparable to those of metal-ceramic restorations. However, the cohesive failure (that is, chipping) of porcelain veneers was identified as the most intractable technical problem affecting such zirconia-ceramic restorations[3, 4]. Relatedly, implant-supported zirconia-ceramic restorations have been found to exhibit significantly higher veneer chipping rates than implant-supported metal-ceramic restorations[1, 5, 6, 7].

The causes of veneer chipping are still uncertain. Many factors have been suspected of being associated with veneer chipping. These factors include the bond strength between the zirconia core and the porcelain veneer, residual thermal stress, occlusal wear damage, the crown geometry (that is, the framework design and relative thickness), and the material of the porcelain veneer, among others[1, 3, 8]. It is believed that veneer chipping is a multifactorial phenomenon.

The crown geometry including the framework design and relative core/veneer thickness is one parameter that dentists can control. Since the optimization of the zirconia cores used in zirconia-ceramic restorations with anatomically supported designs has been proven to reduce veneer chipping[9, 10], there is some question as whether the design of the relative thickness in the zirconia-ceramic restorations could affect their clinical performance. Several in vitro studies have shown that different core and veneer thicknesses in zirconia-ceramic restorations have an influence on their hardness, fracture resistance, fracture toughness, and residual stress[11, 12, 13, 14, 15].

Esquivel-Upshaw et al.[16] evaluated several design parameters including core/veneer thickness ratios, gingival connector embrasure designs, and the connector heights of implant-supported zirconia-ceramic and metal-ceramic fixed dental prostheses in a randomized clinical trial. Although no significant associations were reported between these parameters and the survival probability, it was noted that zirconia-ceramic prostheses exhibited more chipping failures with a core/veneer thickness ratio of 1/1, whereas metal-ceramic prostheses exhibited more chipping failures with a core/veneer thickness ratio of 1/3. Such differences have generated interest in exploring this issue further.

Several studies have used finite element analysis to evaluate the influence of different design parameters, especially framework designs, on stress distribution in crown restorations[17, 18, 19, 20, 21]. Anami et al.[19] reported that the geometry and design could affect the stress distribution of zirconia-ceramic crowns. Their study also indicated that the dimensions of the core and veneer layer could result in differences in stress values.

Pross et al.[22] evaluated the effect of veneer layer thickness on stress distribution by using a two-dimensional axisymmetric model of In-Ceram anterior bridges. With veneer layer thicknesses ranging from 0 mm to 1.6 mm, the maximum tensile stress at the bridge surface varied. The lowest maximum tensile stress occurred with a veneer thickness of 0.4 mm. Moreover, when the veneer layer thickness was less than 0.2 mm or greater than 1 mm, the maximum tensile stress exceeded the yield strength of the veneer porcelain. This indicated that an optimal core/veneer thickness ratio might exist to minimize the stress magnitude and reduce veneer fracture.

Furthermore, Anusavice et al.[23] reported that the different core/veneer thickness ratios and load orientations in bilayered lithium-disilicate-based ceramic crowns have an impact on their time-dependent fracture probability. As the core/veneer thickness ratio was increased, the time-dependent fracture probability decreased. These studies indicated that core/veneer thickness ratios could have an influence on the stress fields affecting all-ceramic restorations.

However, little information regarding the effects of individual designs of different core/veneer thickness ratios on stress distribution in zirconia-ceramic crowns has been made available. Thus, the purpose of this study was to use finite element analysis to evaluate the effect of different core/veneer thickness ratios on stress distribution in implant-supported zirconia-ceramic posterior crowns.

Material and methods

ANSYS software (ANSYS 14.5, ANSYS, Canonsburg, PA, USA) was used to generate the three-

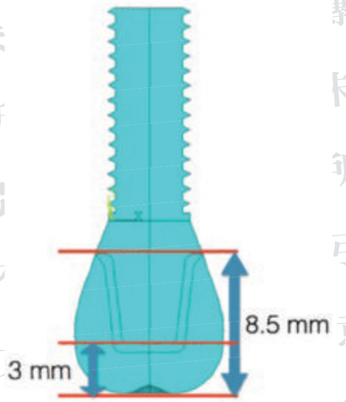

Fig 1. Dimensions of zirconia-ceramic crown

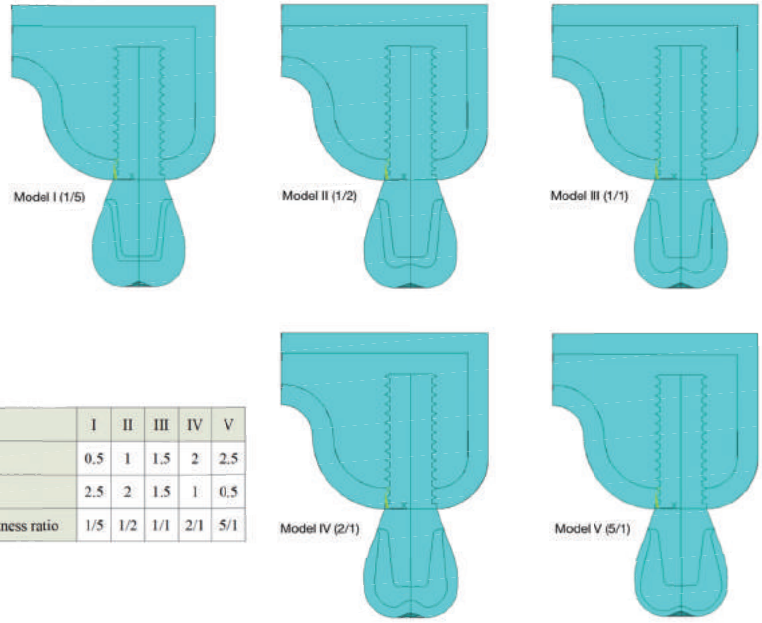

Model	I	II	III	IV	V
Core (mm)	0.5	1	1.5	2	2.5
Veneer (mm)	2.5	2	1.5	1	0.5
Core/veneer thickness ratio	1/5	1/2	1/1	2/1	5/1

Fig 2. Cross-sectional views of the five investigated models

dimensional models, create the mesh of individual elements, and generate the post-processing data needed to calculate the stress of each model. Each model included an implant, abutment, crown, antagonist tooth, and the relevant section of maxillary bone. A maxillary molar was used as a reference to construct the crown.

The geometry of the 13-mm 3i Full OSSEOTITE® Certain® implant (3i, Implant Innovations Inc. Fluoride, U.S.A) was used as a reference to construct the model. The implant was 5 mm in diameter and 13 mm in total length. The abutment was 7.5 mm in height with a 2 mm collar height, and the emergence profile was 6.5 mm. For convenience in terms of the model construction, the anatomic shape of the maxillary molar was simplified. The overall dimensions of the zirconia-ceramic crown from the margin of the abutment to the top of the crown was 8.5 mm in height and 9 mm in width (Fig. 1). The thickness of the crown was 3 mm at the occlusal surface. Five models with different core thicknesses and veneer layer thicknesses in the cusp area were constructed, but all the models were the same in terms of their outer shape (Fig. 2). Specifically, five models with the following different core/veneer thickness ratios were used: model I – 1/5, model II – 1/2, model III – 1/1, model IV – 2/1, and model V – 5/1.

The bone-implant interface was assumed to be completely osseointegrated. In addition, the interfaces between the veneer layer, core layer, abutment, and implant were all assumed to be perfectly bonded. The material properties of all the materials were known from the literature[21, 24, 25]. The cortical and cancellous bones were considered to be homogenous, anisotropic, and linearly elastic. The implant, abutment, zirconia-ceramic crown, and opposite tooth were also considered to be homogeneous, isotropic, and linearly elastic in the model. All the mechanical properties of the materials are listed in Table 1.

Material	Young's modulus (MPa)		Poisson ratio	Reference
Implant & abutment (Titanium)	110,000		0.35	Chang CL et al.[24]
Core (zirconia)	210,000		0.3	Chang CL et al.[24]
Veneer (porcelain)	65,000		0.23	Sung M et al.[21]
Cortical bone	Ex 17900 Ey 12500 Ez 26600	Gyx 4500 Gyz 5300 Gxz 7100	v_{yx}0.18 v_{zy}0.31 v_{xz}0.28	Chang CL et al.[24]
Cancellous bone	Ex 1148 Ey 21 Ez 1148	Gyx 68 Gyz 68 Gxz 434	v_{yx}0.055 v_{zy}0.055 v_{xz}0.322	Chang CL et al[24]
Enamel	84,100		0.33	Dejak B et al.[25]

Table 1. Mechanical properties of the materials

The 10-node tetrahedral solid 187 element and 4-node shell 181 element were used in the study. The pairs of contact elements (target 170 and contact 174) were used at the occlusal surface of each examined crown and opposite tooth. The coefficient of friction between the contact surfaces was assumed to be 0.2[25]. The models were constrained on all nodes of the mesial and distal external surfaces of bone segment in all directions.

The contact analysis method was used in this study, and two different loading conditions were assumed. Both axial loading and oblique loading were applied a motion to maximal intercuspal position. For the axial loading, the nodes on the bottom of the opposite tooth were moved along the y-axis until a reaction force of 300N was achieved. As for the oblique loading, the nodes on the bottom of the opposite tooth were applied along the x-axis and y-axis to produce a reaction force of 350N. The contact simulation of the FEA entailed a nonlinear analysis that required the load and displacement to be applied in a number of steps. Automatic time stepping was applied in this analysis.

The contour plots of the stress distribution, including von Mises stress and the 1st principal stress (tensile stress), were used to compare the different models. The values of the maximum von Mises stress and maximum 1st principal stress for each model were utilized in histograms in order to compare the models.

Results

The accuracy of the model was verified by convergence test. The elements of all the models investigated in the study were between 88993 and 100567. As for the nodes, they were all between 115060 and 130614.

Results of axial loading

The pattern of stress distribution among the five models was similar (Fig. 3). The maximum von Mises stress values applied to the cortical bone, cancellous bone, and implant did not differ significantly. For model V, however, the peak von Mises stress values in the veneer and core layer were significantly greater than those for the other models.

In the veneer layer, the 1st principal stress was localized around the contact area in all five models. When viewed as a cross-section, it could be seen that the 1st principal stress was more dispersed in model I compared to the other four models. As for the core layer, stress concentration beneath the contact areas was more obvious as the core/veneer thickness ratio increased. The peak value in model V was greater than those in the other models (Figs. 4, 5).

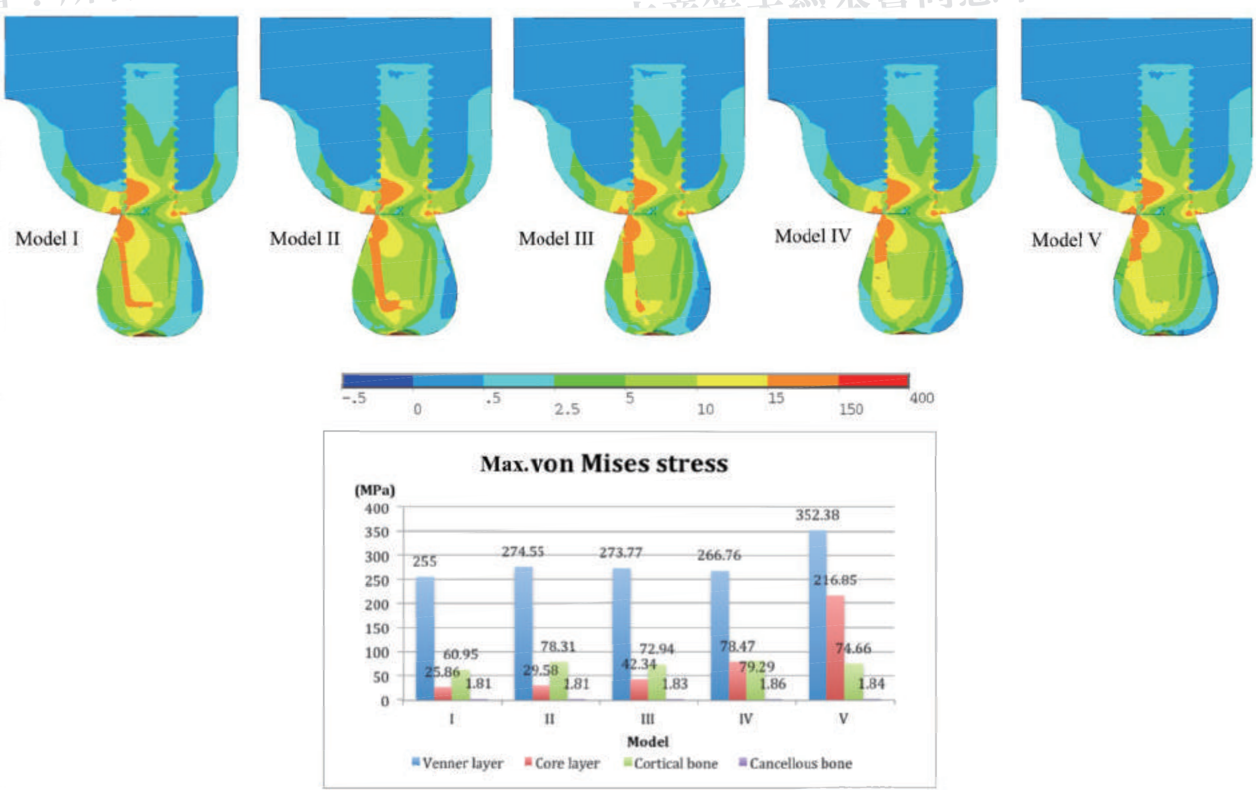

Fig 3. Axial loading—von Mises stress of main model and maximum value

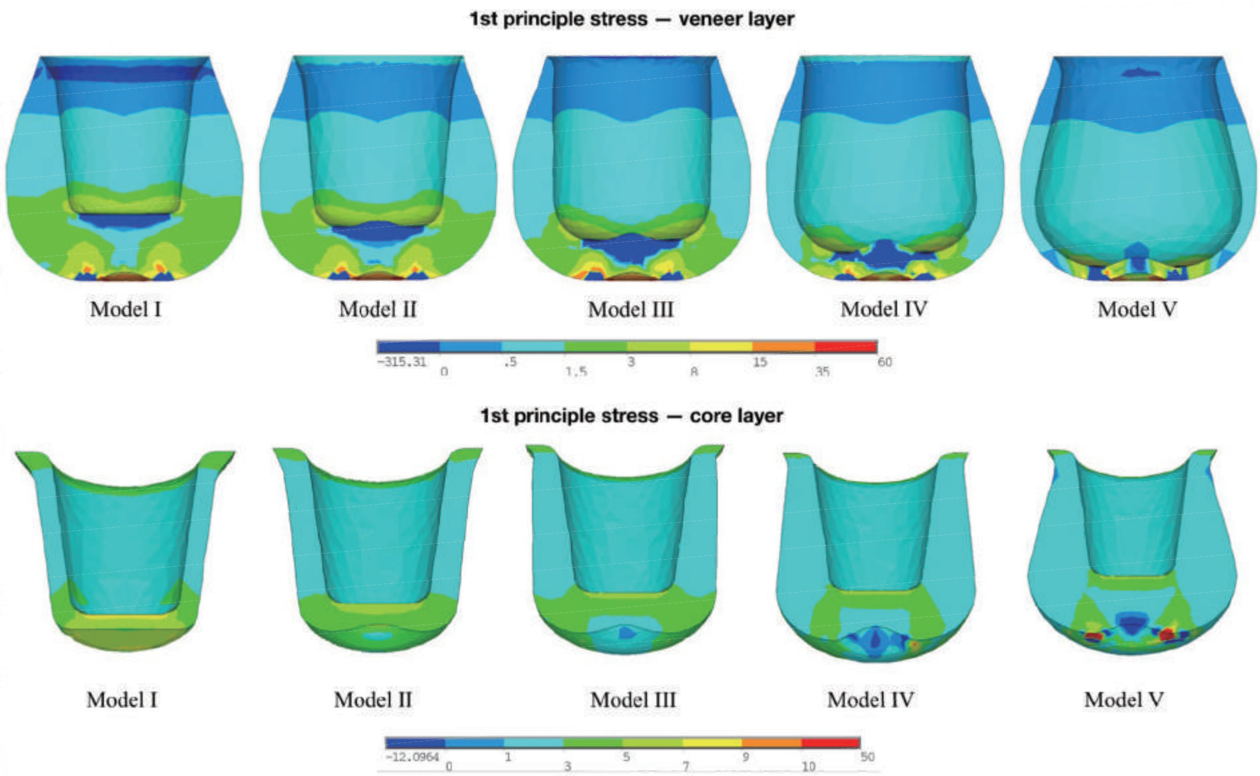

Fig 4. Axial loading—1st principal stress in the core and veneer layer

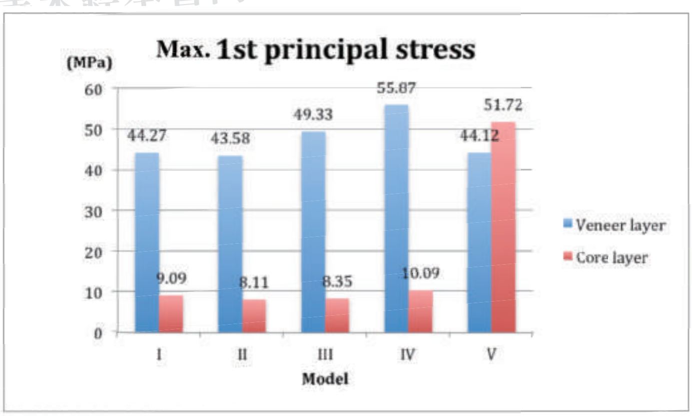

Fig 5. Axial loading—maximum 1st principal stress in the core and veneer layer

Results of oblique loading

The pattern of von Mises stress was similar in all five models (Fig. 6). In model V, both the veneer layer and core layer had significantly greater peak values than the other models. In addition, the peak value of the veneer layer was lower in model III and model IV.

The maximum 1st principal stress in the veneer layer was also located around the contact area in all five models. From the cross-sectional view, it could be seen that compressive stress was concentrated in the contact area and the veneer core interface beneath it. The peak value was greatest in model I and slightly decreased as the veneer thickness decreased. The maximum 1st principal stress in the core layer was located at the cervical margin opposite to the loading direction. The peak value of the maximum 1st principal stress in the core layer of model V was significantly greater than that in the other models (Figs. 7, 8).

Discussion

It is well known that ceramic material is less resistant to tensile stress[17]. With a finite element analysis, it is possible to determine from the stress concentration areas where a

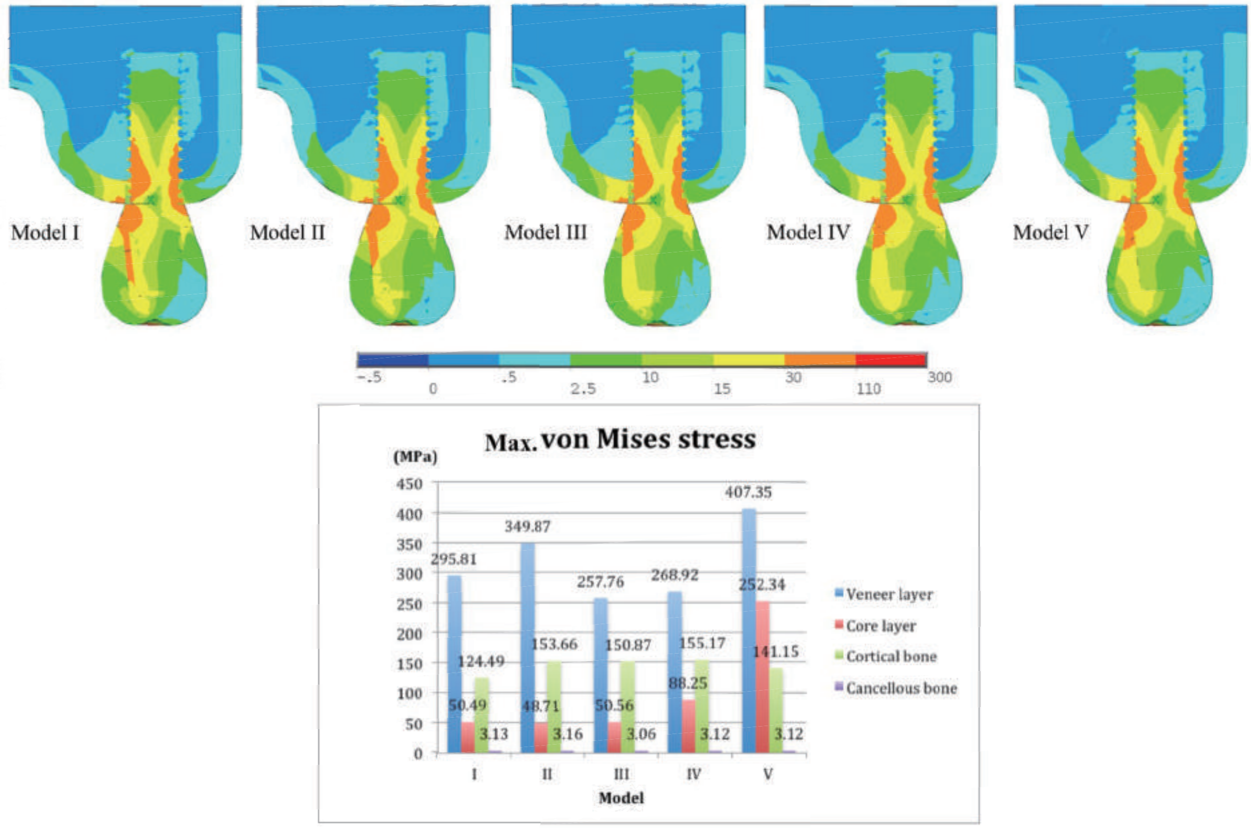

Fig 6. Oblique loading—von Mises stress of main model and maximum value

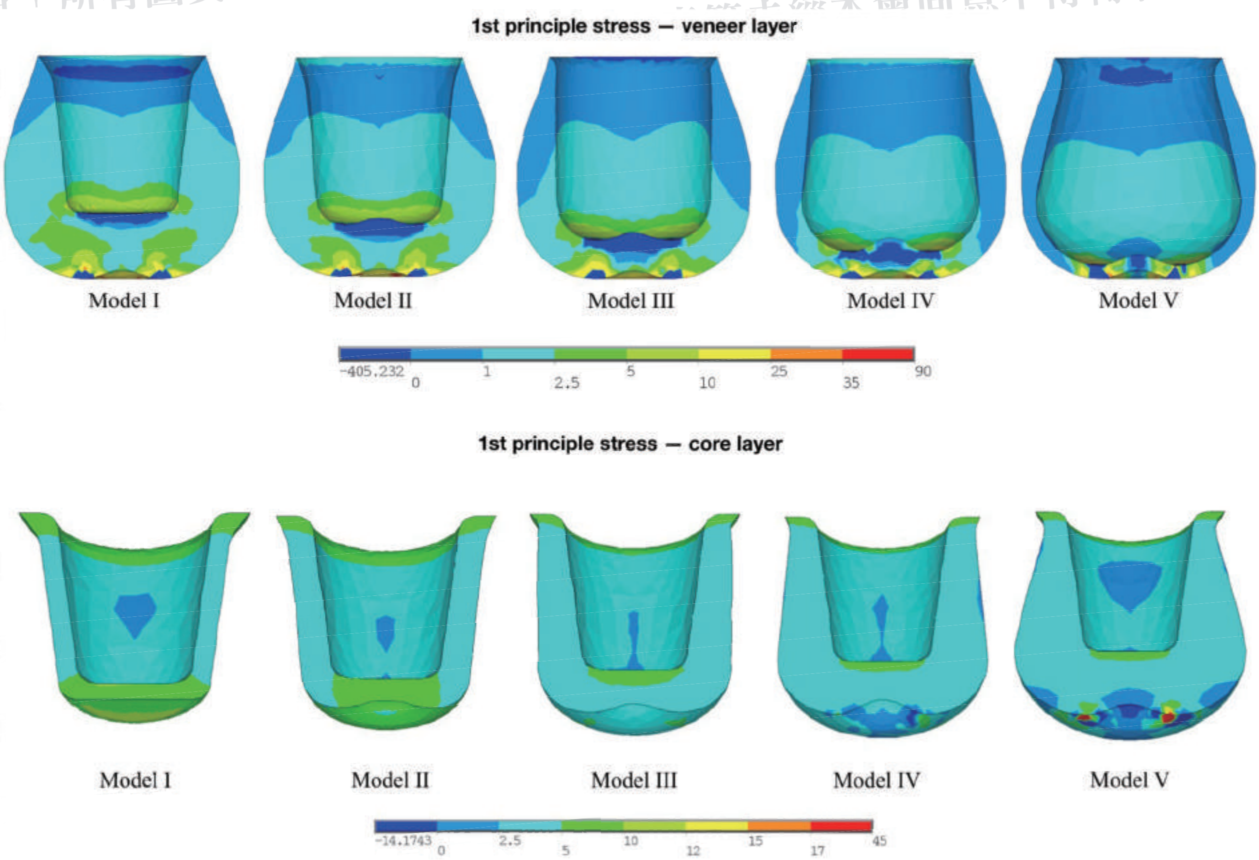

Fig 7. Oblique loading—1st principal stress in the core and veneer layer

fracture could begin. Therefore, the finite element method was used in the present study to provide information that could potentially be used to improve crown designs.

The loading conditions of a finite element model have certain effects on the stress distribution pattern. Previous studies have mostly used linear elastic models, such as those in which force is applied onto a node or an element or pressure is applied onto an occlusal surface to simulate occlusal loading. The above loading condition will lead to excessively concentrated stress peripherally around the loading site[26, 27]. Consequently, it is necessary to remove the singularity during the post processing. In the current study, the purpose was to evaluate the stress distribution patterns in the investigated crowns. However, the fractographic analysis of clinical failed restorations indicated that the fractures mostly originated from the occlusal contact area. As such, it can be concluded that using a linear elastic model may lead to erroneous interpretations of stress distribution patterns in a crown surface. In the studies of Dejak B et al.[25], a cuboid bolus was used to simulate the clinical situation. Nevertheless, the veneer porcelain at the occlusal surface of the crown will be in contact with the opposing dentition during chewing. Consequently the masticatory stress generated during chewing is directly applied on the veneer porcelain in the occlusal region. Thus, contact analysis was used in current study but a food bolus was not simulated.

Since the first molar is located at the center of occlusal loading and withstands the greatest amount of occlusal force, a maxillary first molar was constructed to evaluate the stress state. The human molar bite force ranges from 176N to 750N[28]. In the current study, the axial loading and oblique loading were 300N and 350N, respectively, values which are within the range of normal bite force. In addition, the maximum intercuspation contacts have previously been reported to be significantly associated with the fracture of implant-supported prostheses[29]. Thus, maximum intercuspation contact was assumed in the present study.

In the current study, the von Mises stress magnitude in the supporting bone structures under oblique loading was greater than under axial loading. This result was in accordance with the findings of a previous study[30], which indicated that the oblique load could lead to unfavorable stress concentrations in supporting bone substructures. Therefore, the establishment of an occlusal scheme to reduce lateral occlusal force is recommended in implant-supported restorations.

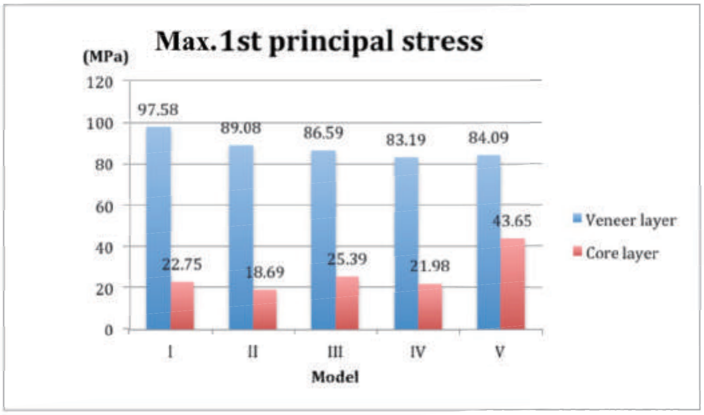

Fig 8. Oblique loading—maximum 1st principal stress in the core and veneer layer

Under axial loading, the maximum 1st principal stress in the core layer significantly increased in model V, although there was no significant difference in the veneer layer. Moreover, from the cross-sectional view it was obvious that the compression stress was concentrated along the contact area and continued to the underlying core layer. This indicated that the veneer layer could not dissipate stress and thus led to significantly increased stress magnitude in the core layer compared to the other four models. This situation was particular obvious in model V with respect to the von Mises stress fields. This indicated that model V, with its core/veneer thickness ratio of 5/1, might undergo the most unfavorable conditions in terms of stress distribution under axial loading.

As for oblique loading, the greatest maximum 1st principal stress in the core layer was also exhibited in model V, just as with axial loading. However, in the veneer layer, model I exhibited the greatest stress magnitude of all the models. Meanwhile, model V had significantly higher maximum von Mises stress values in the core and veneer layer than the other models. In contrast, model III and model IV had lower stress magnitudes. This indicated that the core/veneer thicknesses of 1/1 and 2/1 were more favorable designs under oblique loading.

From the cross-sectional view of the 1st principal stress distribution in crown, it was observed that as the core/veneer thickness ratio was increased, the stress was more concentrated in either loading condition. Meanwhile, although the stiffer zirconia core could assist in allowing the stress to dissipate, the concentrated stress was nonetheless apparent in model V, which had the thinnest veneer thickness compared to the other models. Such stress concentration could lead to the initiation of fractures in the veneer porcelain.

In the present study, the cement layer was not simulated. Rekow et al.[31] evaluated the relative contributions of the variables in a crown-cement-tooth system that can influence the magnitude of maximum principal stress in all-ceramic crowns. Those variables included the crown material, geometry (thickness and cuspal incline), cement modulus and thickness, supporting tooth core, and occlusal loading position. The results of the study showed that the crown material and thickness are of primary importance in stress magnitude. Meanwhile, a study by Kurtoflu C et al.[32] showed that cement thickness had a minor influence on the maximum stress value in ceramic-cement-dentin multilayer systems. However, the ceramic type and thickness had significant impacts on the maximum principal stress value. Wimmer T et al.[33] also found that the Young's modulus of the cement layer only affected the maximum principal stress values in the cement layer. In addition, neither the Young's modulus nor the thickness of the cement layer influenced the displacement and stress distribution of prostheses. Shahrbaf et al.[34] also reported that the elastic modulus of cement did not affect the stress state in the crown and supporting structure of a crown-tooth system. Meanwhile, because the purpose of the current study was to evaluate the individual effect of different core/veneer thickness ratios, the cement layer was negligible.

In the process of zirconia-ceramic restorations, a mismatch of the thermal expansion coefficient and the thermal gradient of cooling will lead to the development of residual stress. Such residual stress could lead to unstable cracking or chipping of porcelain veneer. Swain et al.[35] used a mathematical model to determine that a thicker veneer layer on a zirconia core will generate higher residual stress. Guazzato et al.[36] also pointed out that spontaneous cracking in porcelain/zirconia structures increases with increasing veneer layer thickness. In addition, studies have reported that the magnitude of residual stress is increased with increased veneer layer thickness[37, 38]. However, the effect of residual stress was not taken into account in the present study. Thus, the maximum stress values observed in this study should not be directly compared with other laboratory results; rather, the results in this study should only be compared with each other.

Only a convergence test was conducted to verify the accuracy of the finite element model used in the current study. However, further in vitro validation of the finite element model will improve its reliability and could allow for direct comparison with the results of other studies.

In the current study, a total occlusal thickness of 3 mm was used in five different core/veneer thickness ratios to evaluate the stress distribution pattern under mechanical loading. A further study will be aimed at investigating the effects of other total occlusal thicknesses, such as 2 mm, as well as other restoration materials. In addition, the interactions between thermal residual stress and the core/veneer thickness ratios should be taken into consideration to provide clinicians with more reliable design guidelines in making crown restorations.

Conclusion

The limitations of the present study notwithstanding, the following conclusions were reached:

1. The different core/veneer thickness ratios of zirconia-ceramic crowns have an influence on the stress distributions in such crowns but not on the stress distributions of the implant component or bone structures.
2. Under axial loading, a core/veneer thickness ratio of 5/1 is unfavorable in terms of stress distribution.
3. Under oblique loading, core/veneer thickness ratios of 1/1 and 2/1 are comparatively favorable in terms of stress distribution.

References

1. Guess PC, Schultheis S, Bonfante EA, Coelho PG, Ferencz JL, Silva NR. All-ceramic systems: laboratory and clinical performance. Dent Clin North Am 2011; 55(2): p. 333-52, ix.
2. Ozkurt Z, Kazazoglu E. Clinical success of zirconia in dental applications. J Prosthodont 2010; 19(1): p. 64-8.
3. Silva NR, Sailer I, Zhang Y, Coelho PG, Guess PC, Zembic A, Kohal RJ. Performance of zirconia for dental healthcare. Materials 2010; 3(2): p. 863-896.
4. Larsson C, Wennerberg A. The clinical success of zirconia-based crowns: a systematic review. Int J Prosthodont 2014; 27(1): p. 33-43.
5. Guess PC, Att W, Strub JR. Zirconia in fixed implant prosthodontics. Clin Implant Dent Relat Res 2012; 14(5): p. 633-45.
6. Schwarz S, Schroder C, Hassel A, Bomicke W, Rammelsberg P. Survival and chipping of zirconia-based and metal-ceramic implant-supported single crowns. Clin Implant Dent Relat Res 2012; 14 Suppl 1: p. e119-25.
7. Augstin-Panadero R, Fons-Font A, Roman-Rodriguez JL, Granell-Ruiz M, del Rio-Highsmith J, Sola-Ruiz MF. Zirconia versus metal a preliminary comparative analysis of ceramic veneer behavior. Int J Prosthodont 2012; 25(3): p. 294-300.
8. Zarone F, Russo S, Sorrentino R. From porcelain-fused-to-metal to zirconia: clinical and experimental considerations. Dent Mater 2011; 27(1): p. 83-96.
9. Rosentritt M, Steiger D, Behr M, Handel G, Kolbeck C. Influence of substructure design and spacer settings on the in vitro performance of molar zirconia crowns. J Dent 2009;

37(12): p. 978-83.

10. Larsson C, Madhoun SE, Wennerberg A, Vult von Steyern P. Fracture strength of yttria-stabilized tetragonal zirconia polycrystals crowns with different design: an in vitro study. Clin Oral Implants Res 2012; 23(7): p. 820-6.
11. Sundh A, Sjögren G. A comparison of fracture strength of yttrium oxide partially stabilized zirconia ceramic crowns with varying core thickness shapes and veneer ceramics. J Oral Rehabil 2004; 31(7): p. 682-8.
12. Alhasanyah A, Vaidyanathan TK, Flinton RJ. Effect of core thickness differences on post-fatigue indentation fracture resistance of veneered zirconia crowns. J Prosthodont 2013; 22(5): p. 383-90.
13. Benetti P, Pelogia F, Valandro LF, Bottino MA, Bona AD. The effect of porcelain thickness and surface liner application on the fracture behavior of a ceramic system. Dent Mater 2011; 27(9): p. 948-53.
14. Millen CS, Reuben RL, Ibbetson RJ. The effect of coping/veneer thickness on the fracture toughness and residual stress of implant supported, cement retained zirconia and metal-ceramic crowns. Dent Mater 2012; 28(10): p. e250-8.
15. Lima JM, Souza AC, Anami LC, Bottino MA, Melo RM, Souza RO. Effects of thickness, processing technique, and cooling rate protocol on the flexural strength of a bilayer ceramic system. Dent Mater 2013; 29(10): p. 1063-72.
16. Esquivel-Upshaw JF, Clark AE, Shuster JJ, Anusavice KJ. Randomized clinical trial of implant-supported ceramic-ceramic and metal-ceramic fixed dental prostheses: preliminary results. J Prosthodont 2014; 23(2): p. 73-82.
17. Esquivel-Upshaw JF, Anusavice KJ. Ceramic design concepts based on stress distribution analysis. Compend Contin Educ Dent 2000; 21(8): p. 649-52, 654; quiz 656.
18. Motta AB, Pereira LC, Duda FP, Anusavice KJ. Influence of substructure design and occlusal reduction on the stress distribution in metal ceramic complete crowns: 3D finite element analysis. J Prosthodont 2014; 23(5): p. 381-9.
19. Anami LC, Lima JM, Corazza PH, Yamamoto ET, Bottino MA, Borges AL. Finite element analysis of the influence of geometry and design of zirconia crowns on stress distribution. J Prosthodont 2015; 24(2): p. 146-51.
20. Kirsten A, Parkot D, Raith S, Fischer H. A cusp supporting framework design can decrease critical stresses in veneered molar crowns. Dent Mater 2014; 30(3): p. 321-6.
21. Sung M, Han CH, Kim S. A novel coping design to decrease maximum principal stress in zirconia ceramic restorations. J Prosthodont 2014; 23(7): p. 534-9.
22. Proos K, Steven G, Swain M, Ironside JIM. Preliminary Studies on the Optimum Shape of Dental Bridges. Computer Methods in Biomechanics and Biomedical Engineering 2001; 4(1): p. 77-92.
23. Anusavice KJ, Jadaan OM, Esquivel-Upshaw JF. Time-dependent fracture probability of bilayer, lithium-disilicate-based, glass-ceramic, molar crowns as a function of core/veneer thickness ratio and load orientation. Dent Mater 2013; 29(11): p. 1132-8.
24. Chang CL, Chen CS, Huang CH, Hsu ML. Finite element analysis of the dental implant using a topology optimization method. Med Eng Phys 2012; 34(7): p. 999-1008.
25. Dejak B, Mlotkowski A, Langot C. Three-dimensional finite element analysis of molars with thin-walled prosthetic crowns made of various materials. Dent Mater 2012; 28(4): p. 433-41.
26. Wakabayashi N, Ona M, Suzuki T, Igarashi Y. Nonlinear finite element analyses: advances and challenges in dental applications. J Dent 2008; 36(7): p. 463-71.
27. Murakami N, Wakabayashi N. Finite element contact analysis as a critical technique in dental biomechanics: a review. J Prosthodont Res 2014; 58(2): p. 92-101.
28. Misch CE. Contemporary Implant Dentistry. 3rd ed. 2008.
29. Esquivel-Upshaw JF, Mehler A, Clark AE, Neal D, Anusavice KJ. Fracture analysis of randomized implant-supported fixed dental prostheses. J Dent 2014; 42(10): p. 1335-42.
30. Sotto-Mario BS, Mendes Senna P, da Silva WJ, Rocha EP, Del Bel Cury AA. Influence of crown-to-implant ratio, retention system, restorative material, and occlusal loading on stress concentrations in single short implants. Int J Oral Maxillofac Implants 2012; 27(3): p. e13-8.
31. Rekow ED, Harsono M, Janal M, Thompson VP, Zhang G. Factorial analysis of variables influencing stress in all-ceramic crowns. Dent Mater 2006; 22(2): p. 125-32.
32. Kurtoglu C, Uysal H, Mamedov A. Influence of layer thickness on stress distribution in ceramic-cement-dentin multilayer systems. Dent Mater J 2008; 27(4): p. 626-32.
33. Wimmer T, Erdelt KJ, Raith S, Schneider JM, Stawarczyk B, Beuer F. Effects of differing thickness and mechanical properties of cement on the stress levels and distributions in a three-unit zirconia fixed prosthesis by FEA. J Prosthodont 2014; 23(5): p. 358-66.
34. Shahrbaf S, vanNoort R, Mirzakouchaki B, Ghassemieh E, Martin N. Effect of the crown design and interface lute parameters on the stress-state of a machined crown-tooth system: a finite element analysis. Dent Mater 2013; 29(8): p. e123-31.
35. Swain MV. Unstable cracking (chipping) of veneering porcelain on all-ceramic dental crowns and fixed partial dentures. Acta Biomater 2009; 5(5): p. 1668-77.
36. Guazzato M, Walton TR, Franklin W, Davis G, Bohl C, Klineberg I. Influence of thickness and cooling rate on development of spontaneous cracks in porcelain/zirconia structures. Aust Dent J 2010; 55(3): p. 306-10.
37. Benetti P, Kelly JR, Sanchez M, Della Bona A. Influence of thermal gradients on stress state of veneered restorations. Dent Mater 2014; 30(5): p. 554-63.
38. Zhang Z, Guazzato M, Sornsuwan T, Scherrer SS, Rungsiyakull C, Li W, Swain MV, Li Q. Thermally induced fracture for core-veneered dental ceramic structures. Acta Biomater 2013; 9(9): p. 8394-402.

Original Article

Effect of a Commercial Fluorescence Liquid on 3Y-TZP Surface Microstructure: A Preliminary Study

Jing-Fen Wu, DDS, MS
Graduate Institute of Clinical Dentistry, School of Dentistry, National Taiwan University, Taipei, Taiwan

Tong-Mei Wang, DDS, MS, PhD
Graduate Institute of Clinical Dentistry, School of Dentistry, National Taiwan University, Taipei, Taiwan

Ru-Shi Liu, MS, PhD
Department of Chemistry, National Taiwan University, Taipei, Taiwan

Li-Deh Lin, DDS, PhD
Graduate Institute of Clinical Dentistry, School of Dentistry, National Taiwan University, Taipei, Taiwan

Corresponding author:

Li-Deh Lin, DDS, PhD
Graduate Institute of Clinical Dentistry, School of Dentistry, National Taiwan University, Taipei, Taiwan
No. 1, Chang-Te St, Jhongjheng Dist, Taipei City 100, Taiwan R.O.C.
Fax: +886-2-2383-1346
E-mail: lidehlin@ntu.edu.tw

Abstract

Objective

3 mol% yttrium-stabilized tetragonal zirconia poly-crystal (3Y-TZP) ceramics can be stained with a color/fluorescence liquid to match the color and fluorescence of natural teeth. However, the effects of different shading liquids and methods are still not fully known. The purpose of this study, therefore, was to evaluate the effect of a commercial fluorescence liquid on the surface microstructure of 3Y-TZP ceramics.

Material and methods

Green-stage 3Y-TZP ceramics (Zirkonzahn® Prettau Zirkon) were sectioned into disc forms and divided into 3 groups: the dip-coating (D) group, the brush-coating (B) group, and the control (C) group. The D and B groups were shaded with a commercial fluorescence liquid before sintering either by dipping or by brushing respectively. Undyed discs were used as the C group. Each disc was 10mm in diameter and 2mm in thickness after sintering. X-ray diffraction analysis (XRD) was used to analyze the crystalline forms of each group. Surface structural differences and chemical compositions were evaluated by scanning electron microscopy (SEM) and energy dispersive analysis (EDS). The mean grain size of each group was calculated by the circular intercept method (that is, Abram's Three-Circle Procedure). One-way ANOVA analysis and the Tukey test were used to analyze the data, at a significant level of P Value <0.05.

Results

The XRD results showed that each group was mainly composed of tetragonal phase and a small quantity of monoclinic phase. The SEM results revealed that the different shading methods changed the distribution of the coloring pigment, homogeneity of grain size, and mean grain size. The B group had more even and smaller grains (than the C group, whereas the D group had nonhomogeneous and larger grains). The difference was statistically significant ($p<0.05$).

Conclusion

Shading with a commercial fluorescence liquid by prolonged dipping could result in nonhomogeneous and enlarged grain sizes. It is thus recommended that shading be performed by brushing instead of prolonged dipping in clinical use.

Keywards: crystalline, fluorescence, grain size, 3Y-TZP

Introduction

Fluorescence is the emission of visible light from a substance that occurs when the substance is excited by a shorter wavelength light or radiation. In 1911, Stübel et al.[1-3] first reported that natural teeth emitted bluish fluorescence under UV light. The fluorescence properties of different parts of human teeth are heterogeneous. Human dentin and cementum display more intense fluorescence than enamel[2-4]. Fluorescence makes natural teeth look brighter and whiter[1, 5]. A restoration emitting fluorescence can return more light to the observer, lower the chroma, and hide underlying discoloration[5]. Generally, the value of a restoration decreases as the translucency of the restoration increases. For high-value cases, fluorescence emitted from the inner layer of a restoration can increase its value without decreasing its translucency[5]. In clinical practice, rare earth oxides (e.g. europium, cerium, and ytterbium) are usually added into dental porcelain powder and composite resin as phosphors for fluorescence emission[6, 7].

3 mol% yttrium-stabilized tetragonal zirconia poly-crystal (3Y-TZP) ceramics have become one of the most popular restorative materials in recent years due to the excellent mechanical properties, good biocompatibility, and tooth-like ivory/white color appearance of 3Y-TZP. However, pure 3Y-TZP ceramics are still too white and opaque to meet clinical esthetic demands. As such, the application of shading to 3Y-TZP ceramics is one solution for improving the esthetic performance of these ceramics. There are two available methods for shading 3Y-TZP ceramics[8, 9]. The first method consists of adding pigments into the ceramic powder before the powder is pressed into green-stage 3Y-TZP milling blanks. The pigments are thus homogeneously distributed in the milling blanks. The other method consists of the use of colored liquids to stain green-stage 3Y-TZP ceramics before subjecting them to the sintering process. These colored liquids can be applied by brushing or dipping. In addition to these colored liquids, some manufacturers also provide a fluorescence liquid that can be applied to 3Y-TZP ceramics to cause them to mimic the photoluminescence of natural teeth. Dental technicians can adjust the color or fluorescence by changing the painting strokes or immersion time they use when applying the liquid to the ceramics. However, the effects of different application methods and colored liquids on 3Y-TZP ceramics are still not entirely clear.

The purpose of this preliminary study is thus to evaluate the effects of a commercial fluorescence liquid and different application methods on the surface microstructure of 3Y-TZP ceramics.

Material and methods

Sample preparation

Green-stage 3Y-TZP (Zirkonzahn® Prettau Zirkon) blanks were milled into disc forms by a milling machine (Zirkonzahn® CAD/CAM System 5-TEC). A commercial fluorescence liquid (Zirkonzahn®) was then applied to some of the 3Y-TZP discs to increase their fluorescence, while one group of discs was left undyed. Each specimen that was stained was stained using just one of the following two shading methods: dipping or brushing. Thus, the discs were effectively divided into 3 groups: the control group (C) (that is, the undyed discs), the dip-coating group (D), and the brush-coating group (B). The C group discs (n=3) were, again, prepared without any shading. For the D group, the discs (n=4) were immersed in the fluorescence liquid for 10 min. For the B group, the fluorescence liquid was applied on the surface of the discs (n=4) with a metal-free brush. After the staining procedure, the specimens were dried under infra-red lamp for 45 minutes. Then the specimens were sintered in a sintering oven (Zirkonzahn®) at 1600°C for 2 hours. After the sintering process, each disc was 10mm in diameter and 2mm in thickness.

X-ray diffraction analysis

The crystalline phases of the C, D, and B groups were analyzed by X-ray diffraction analysis (XRD) using a 30kV, 10mA Cu-K α X-ray. Each scan was performed with the following settings: a 2θ angle of between 20°-90°, a step size of 0.02°, and a time step of 0.9sec (Bruker D2 PHASER).

The acquired diffraction data of the specimens were compared with the crystallographic database of the Powder Diffraction File™ (PDF®). The matched diffraction patterns were found to identify the crystalline phases of the specimens.

Scanning electron microscope

The specimens then were coated with a layer of 10 to 20 nm-thick Pt-Au before being subjected to scanning electron microscopy (SEM) examinations. The topographic images of the specimens were recorded by a field emission scanning electron microscope (JOEL JSM-6700F SEM). The average grain size was calculated by the circular intercept method (that is, Abram's Three-Circle Procedure). The data was analyzed by one-way ANOVA analysis and the Tukey test, at a significant level of P Value <0.05. The surface chemical composition of the specimens was determined by X-ray energy dispersive spectrometer (EDS).

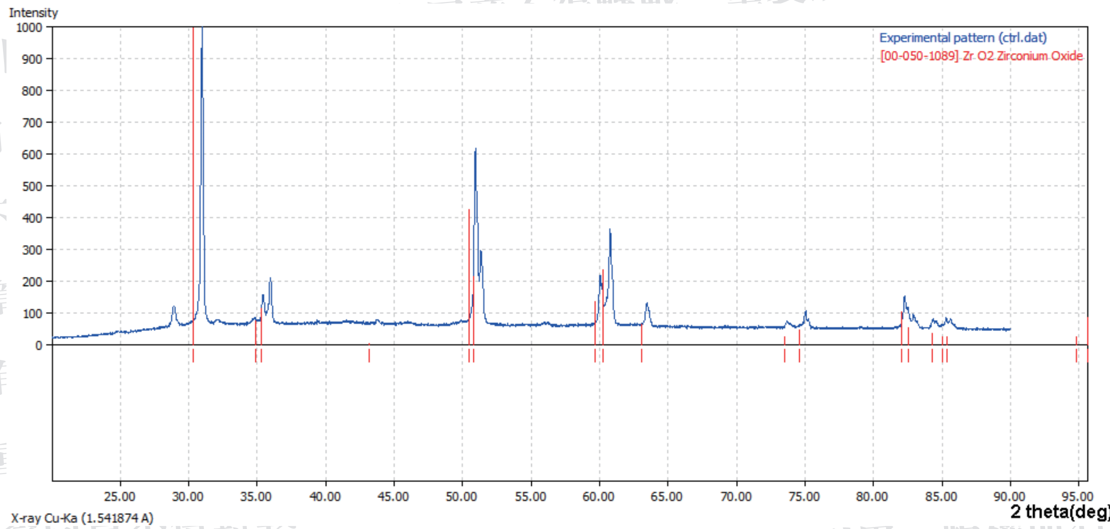

Fig. 1: XRD spectrum of undyed 3Y-TZP (C).

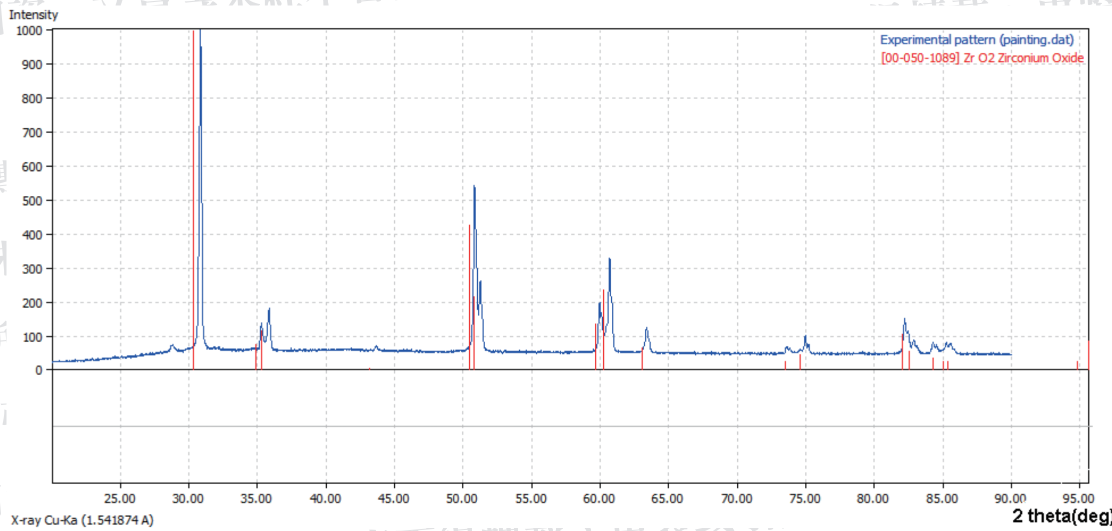

Fig. 2: XRD spectrum of 3Y-TZP shaded by brushing (B).

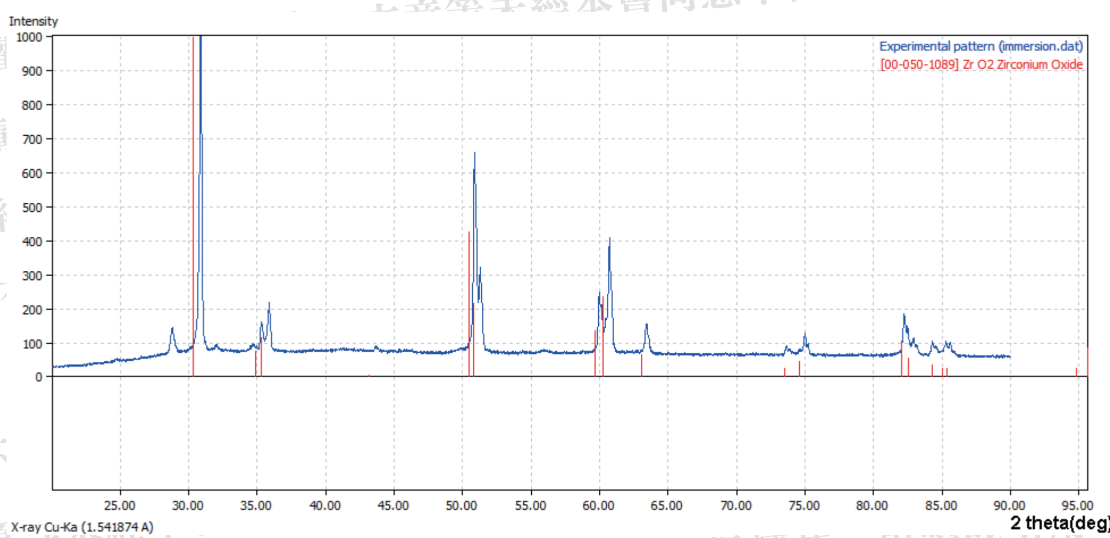

Fig. 3: XRD spectrum of 3Y-TZP shaded by dipping (D).

Results

X-ray diffraction analysis

Figures 1-3 show the individual XRD data and a matched spectrum of the C, D, and B groups. The blue line in each figure presents the diffraction data of each group. The red line indicates a matched standard diffraction spectrum for each group, and the results revealed that all the groups had the same matched spectrum – tetragonal phase. That is, the XRD data showed that the discs in all the groups were mainly composed of tetragonal phase. Compared to the C group discs, however, the diffraction peaks of the B and D groups were left shifted. This shift in the diffraction peaks indicated changes of in the lattice parameters of the B and D group discs relative to the C group discs.

For each group, there were two additional weak diffraction peaks, m(-1,1,1) and m(1,1,1,), observed at 2θ between 28° and 32° (Fig. 4), and these peaks belonged to the monoclinic phase. These weak diffraction peaks thus indicated that each group contained traces of monoclinic phase.

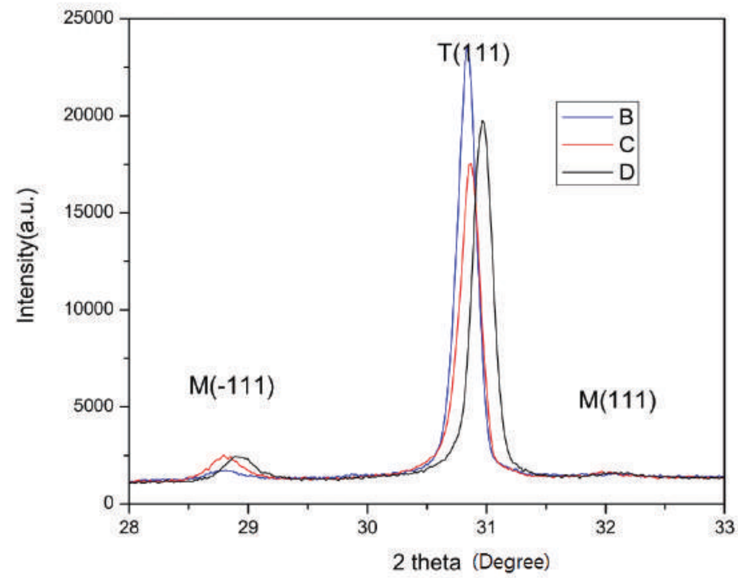

Fig. 4: Monoclinic phase contents was found in all three groups.

Scanning electron microscope

The SEM images revealed that the C group discs simply contained ZrO_2 grains of homogeneous grain size (Fig. 5). The mean grain size of the C group discs was μm. The B and D group discs (Figs. 6 and 7) were mainly composed of ZrO_2 grains, although their surfaces were covered with other particles. There were three different kinds of particles other than ZrO_2 grains noted. The grain size of the ZrO_2 grains in the B group discs was homogeneous, and the mean grain size was . The D group discs had more variable ZrO_2 grain dimensions and a mean grain size, μm, that was larger than the mean grain sizes of the C and B groups. The difference was statistically significant ($p<0.05$).

The EDS results showed that the C group discs mainly contained the elements of zirconium and oxygen. In addition to zirconium and oxygen, a remarkable amount of carbon was found in the D and B group discs.

Discussion

At atmospheric pressure, pure zirconia can exist in three different crystallographic forms – the monoclinic phase, tetragonal phase, and cubic phase - as temperature rises. The equilibrium phase at room temperature is the monoclinic phase. As the temperature rises to 1170℃, zirconium transforms into the tetragonal phase, and at 2370℃, it trans-

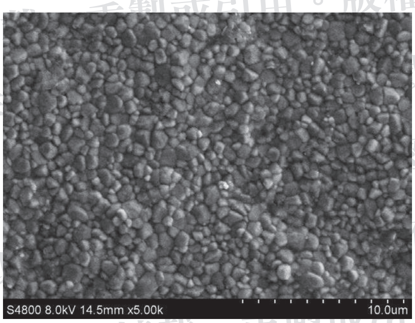

Fig. 5: SEM image of undyed 3Y-TZP (C), 5000x magnification.

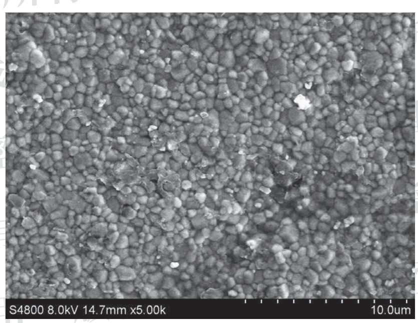

Fig. 6: SEM image of 3Y-TZP shaded by brushing (B), 5000x magnification.

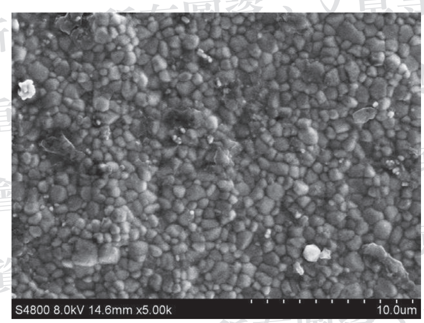

Fig. 7: SEM image of 3Y-TZP shaded by dipping (D), 5000x magnification.

forms into the cubic phase. Zirconium in its monoclinic phase has low strength and toughness. When alloying with some dopants such as MgO, CaO, and Y_2O_3, zirconium can maintain its tetragonal or cubic phase at room temperature. Under such circumstances, it is in a metastable state, and stress can break the stability and provoke its transformation. This kind of stress-induced transformation, from the tetragonal phase to the monoclinic phase, leads to an approximately 4.5% increase in the volume of the zirconium. This volume increase can result in compressive stress and prevent crack propagation. This is the phase transformation toughening (PTT) mechanism that gives dopant-stabilized tetragonal zirconia poly-crystal (TZP) ceramics their extremely excellent mechanical properties[10-12].

3Y-TZP is a material of high flexural strength and fracture toughness. It is composed of fine grain zirconia, containing both the monoclinic and tetragonal phases with a very high content of the metastable tetragonal phase. It was reported by Gupta et al. that the flexural strength of 3Y-TZP is increased as its tetragonal phase content is increased, whereas it is decreased as the monoclinic phase content is increased[13]. Lange et al. observed that the fracture toughness of 3Y-TZP is also correlated with its tetragonal phase content[14]. In summary, the mechanical properties of 3Y-TZP are directly related to its tetragonal phase content.

In this study, the XRD results revealed that the tested commercial 3Y-TZP samples in all three groups were mainly composed of tetragonal phase with a small portion of monoclinic phase, even after groups B and D were shaded with a fluorescence liquid using different methods. The fraction of monoclinic phase can be calculated using the Garvie-Nicholson formula. It showed that the group D discs had higher monoclinic phase content than the other groups. This increased monoclinic phase content after shading by prolonged dipping may be accompanied by lowered strength and toughness. However, the ability of XRD as a tool for detecting small fractions (< 5%) has certain limitations. Further investigations would thus be necessary to provide a reliable evaluation in this regard.

In humid environments, the surface of 3Y-TZP may spontaneously undergo a slow phase transformation that is known as low temperature degradation (LTD) or aging. This kind of transformation leads to surface roughening or micro-cracking. PTT and LTD are both based on the same mechanism, the transformation of a thermodynamically metastable phase. It is thus impossible to take advantage of PTT without facing the risk of LTD.

The stability of a zirconium metastable phase is affected by its grain size. As the grain size is decreased, zirconium becomes more stable in its tetragonal phase. As the grain size is increased, zirconium becomes more stable in its monoclinic phase. Lange et al. reported there was a critical grain size for fixed content yttrium-stabilized zirconia poly-crystal. Above the critical grain size, ZrO_2 had a tendency to exist in the monoclinic phase, and below that size, ZrO_2 tended to exist in the tetragonal phase[14]. This phenomenon implied that changes in grain size may be accompanied by changes in toughness. It was also observed that maximum fracture toughness occurred just below the critical grain size[14, 15]. According to the study by Lange et al., the critical grain size of 3Y-TZP was slightly smaller than 1 μm and optimum fracture toughness was obtained. However, LTD is another phenomenon of concern in clinical practice. Studies have shown that the LTD resistance of 3Y-TZP is closely related to its grain size as well. As the grain size is increased above 0.6μm, the LTD resistance decreases obviously[16]. In summary, both the fracture toughness and LTD of 3Y-TZP are critically dependent on the grain size. A balance must therefore be struck between fracture toughness and LTD resistance when deciding the grain size of 3Y-TZP.

In this study, we found that prolonged dipping with a commercial fluorescence liquid would result in enlarged and nonhomogeneous grain size. This result means that prolonged dipping with a fluorescence liquid may lead to a decrease in the LTD resistance. Such a decrease in LTD resistance would, in turn, affect the long-term survival of 3Y-TZP. However, the actual changes in LTD resistance and its implications after shading were not determined in this study. Further investigations are thus needed.

Conclusion

In this study, we found that, compared to the brushing method, shading by prolonged dipping leads to enlarged and heterogeneous grain size, and that the difference was statistically significant ($p < 0.05$). Shading by brushing is thus probably is a better method to use than dipping when seeking to maintain an adequate and even grain size of ZrO_2. However, the physical properties of 3T-TZP after it is subjected to shading with a commercial fluorescence liquid are still not fully known. Further studies are thus necessary to evaluate the effect of a commercial fluorescence liquid on 3Y-TZP.

References

1. Lee YK. Fluorescence properties of human teeth and dental calculus for clinical applications. J Biomed Optics 2015;20(4):040901. Available at: https://doi.org/10.1117/1.JBO.20.4.040901. Accessed March 4, 2018.
2. Hartles RL, Leaver AG. The fluorescence of teeth under

ultraviolet irradiation Biochem J 1953;54:632-8.

3. Horibe H, Katsura S, Fujimori K, Yamada M. Multiple distribution of the fluorescence in human teeth. Acta Histochemica Et Cytochemica 1974;7:334-41.
4. Hoerman KC, Mancewicz SA. Phosphorescence of calcified tissues. Archives Oral Biology 1964;9:517-34.
5. Fondriest J. Shade matching in restorative dentistry: The science and strategies. Int J Periodontics Restorative Dent 2003;23:467-79.
6. Meller C, Klein C. Fluorescence properties of commercial composite resin restorative materials in dentistry. Dent Mater J 2012;31:916-23.
7. Monsenego G, Burdairon G, Clerjaud B. Fluorescence of dental porcelain. J Prosthet Dent 1993;69:106-13.
8. Vichi A, Louca C, Corciolani G, Ferrari M. Color related to ceramic and zirconia restorations: A review. Dent Mater 2011;27:97-108.
9. Oh GJ, Lee K, Lee DJ, et al. Effect of metal chloride solutions on coloration and biaxial flexural strength of yttria-stabilized zirconia. Metals & Materials International 2012;18:805-12.
10. Chevalier J, Gremillard L, Virkar AV, Clarke DR. The tetragonal-monoclinic transformation in zirconia: Lessons learned and future trends. J Am Ceram Soc 2009;92:1901-20.
11. Denry I, Kelly JR. State of the art of zirconia for dental applications. Dent Mater 2008;24:299-307.
12. Kelly JR, Denry I. Stabilized zirconia as a structural ceramic: An overview. Dent Mater 2008;24:289-98.
13. Gupta TK, Bechtold JH, Kuznicki RC, Cadoff LH, Rossing BR. Stabilization of tetragonal phase in polycrystalline zirconia. J Materials Science 1977;12:2421-26.
14. Lange FF. Transformation toughening: Part 3, Experimental observations in the ZrO2–Y2O3 System. J Materials Science 1982;17:240-46.
15. Gupta TK, Lange FF, Bechtold JH. Effect of stress-induced phase transformation on the properties of polycrystalline zirconia containing metastable tetragonal phase. J Materials Science 1978;13:1464-70.
16. Munoz-Saldana J, Balmori-Ramirez H, Jaramillo-Vigueras D, Iga T, Schneider GA. Mechanical properties and low-temperature aging of tetragonal zirconia polycrystals processed by hot isostatic pressing. J Materials Research 2003;18(10):2415-26.

Case Report

Application of Palatal Augmentation Prostheses for a Patient with Partial Glossectomy

Wan-Ting Chang, DDS
Attending Doctor, Dental Department
Ditmanson Medical Foundation
Chia-yi Christian Hospital,
Chiayi Taiwan

Chung-Hsiao Cheng, BDS
Director, Department of prosthodontics
Taichung Veterans General Hospital,
Taichung Taiwan

Corresponding author:

Chung-Hsiao Cheng, BDS
Director, Department of Prosthodontics
Taichung Veterans General Hospital,
Taichung Taiwan
No.1650 Taiwan Boulevard Sect. 4,
Taichung City, Taiwan R.O.C.
Tel: +886-4-2359-2525 ext. 5520
Fax: +886-4-2359-5046
E-mail: cheng1448@yahoo.com.tw

Abstract

The swallowing and chewing of patients who undergo a partial glossectomy to treat oral cancer or for other reasons are affected according to the size of the excision. Damage inflicted upon the lingual nerves by the procedure is also a factor. The use of palatal augmentation prostheses (PAPs) can help patients to improve the functions of phonation and food consumption by increasing contact between the tongue and the palatal surface of the prostheses during swallowing. This clinical report details the treatment provided to a patient who received a partial glossectomy due to squamous cell carcinoma (SCC). The intraoral status of the patient was defined by a fully edentulous ridge with limited tongue movement. After the palatal augmentation prosthesis was delivered, the patient adapted well to it and his chewing function was improved. The 2-year follow-up showed no obvious complications.

Key words: glossectomy, palatal augmentation prostheses

Introduction

The palatal augmentation prosthesis (PAP) was first reported in the literature by Cantor et al.[1] Prostheses of this type benefit people whose tongue is totally or partially resected, resulting in problems with dysarthria and dysphagia. In normal people, functional contacts occur between the tongue and palate allow them to complete the swallowing process.

Swallowing can be separated into 3 phases, namely, the oral, pharyngeal, and esophageal phases[2]. Factors affecting any of those phases can result in dysphagia. Relatedly, the surgical excision of oral pathological lesions will influence the oral phase of swallowing. Following a glossectomy, bolus tranportation from the oral cavity to the pharynx becomes weak and the tongue base pressure decreases. A PAP is a prosthesis that helps people with tongue dysfunction by reshaping the hard palate to improve the contact between the tongue and palate[3]. The palatal vault will become lower within a PAP so that the tongue to palate distance is decreased, benefiting people whose tongue mobility is impaired.

Psychological and sociological adaptation to a PAP is also an important issue[4]. The size of an excision, as well as the extent and location of any defects, affect the degree of impairment of the tongue. In addition, radiation therapy or other ablative procedures are frequently used in combination patients who undergo a partial or total tongue resection. The functions of swallowing and aspiration will be affected

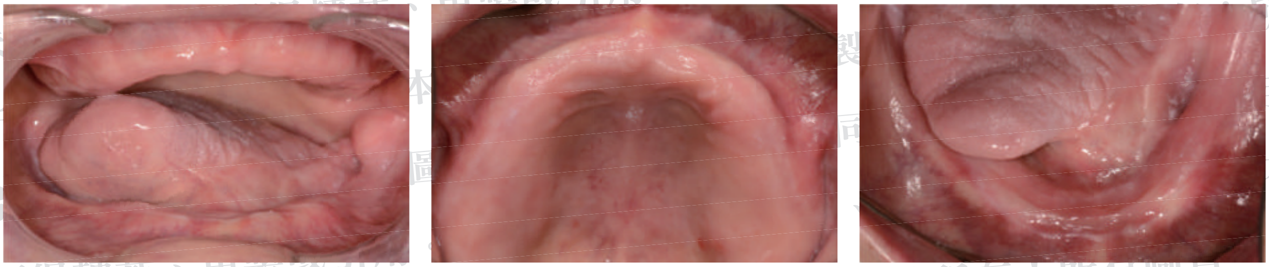

Fig. 1: Patient's maxillary and mandibular edentulous status, frontal and occlusal views

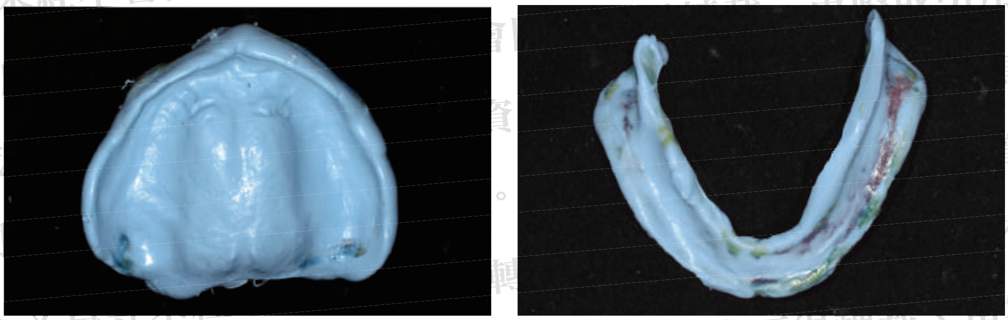

Fig. 2: Maxillary and mandibular impression

by these treatments and the risk of aspiration pneumonia therefore increases[5]. The use of a PAP can assist patients in swallowing safely and efficiently.

The present clinical report focuses on the method of PAP fabrication utilized for a patient who underwent a partial glossectomy.

Case report

A 70-year-old male patient came to the prosthodontic department of VGHTC with the chief complaint that his old complete dentures were severely worn and he could not consume food well. The medical history of the patient included a partial glossectomy 16 years earlier due to squamous cell carcinoma (SCC) over the left tongue border. He also underwent concomitant chemo-radio-therapy.

The intraoral examination revealed that the maxillary edentulous ridge was of good quality but the mandibular ridge was moderately resorbed (Fig. 1). A hyperkeratinized left tongue border was also noted. Moreover, the movement of the patient's tongue was limited, and he experienced difficulty with swallowing.

Due to financial problems, the patient could not afford an implant; therefore, a definitive treatment plan consisting of application of a maxillary PAP and mandibular complete denture was suggested and agreed to by the patient.

The preliminary impressions were taken and custom resin trays were fabricated for final impressions. Green stick compound (PERI COMPOUND, GC Corporation, Japan) was used to conduct the border molding procedures in the same way as conventional complete dentures are fabricated. The final impression was taken with polyvinyl siloxane material (Exadenture tube, GC, Japan) (Fig. 2). After beading and boxing, the master casts were poured.

Trial denture bases and occlusion rims were fabricated on the master casts. The vertical dimension was determined using the same general procedures applied to normal patients, including physiological methods such as testing of the swallowing threshold and phonetics. In addition, centric relation registration was also taken. The master casts were mounted on a semi-adjustable articulator (Artex® CT, Austria) with three remounting indices on each cast. Resin artificial teeth (Bioblend IPN denture teeth, Dentsply, USA) were then arranged as necessary to achieve balanced occlusion.

The trial dentures were fitted and the facial profile was checked with patient. The vertical dimension and centric relation position were confirmed additionally. The dentures were processed with heat-cured resin (Lucitone199, Dentsply, USA). After the laboratory remounting procedure, the occlusion was adjusted again. A clinical remounting jig was made with the adjusted maxillary denture. The dentures


Fig. 3: The processed maxillary and mandibular dentures

Fig. 4-1: No contact of tongue and palatal surface of maxillary denture was noted when patient swallowed

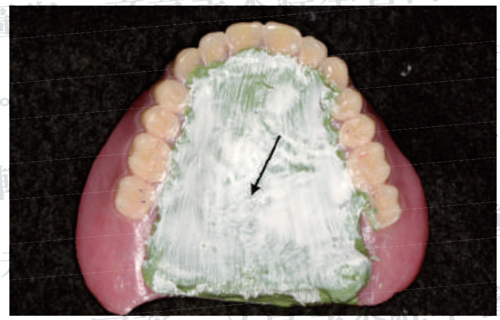

Fig. 4-2: Impression compound application and checking tongue contact with PIP

Fig. 4-3: Impression wax application

Fig. 4-4: Checking with PIP

were removed from the master casts and then the procedures of finishing and polishing were completed.

The denture delivery procedures were arranged with the patient (Fig. 3). The tissue surface and border extension were checked first and occlusion was adjusted with clinical remounting procedures. After that, the fabrication of the PAP was begun. According to the marks on the pressure indicating paste (PIP, National Keystone, USA), no contact between the tongue and palatal area of the denture during swallowing was noticed (Fig. 4-1). At the beginning, the Green stick compound (PERI COMPOUND, GC Corporation, Japan) was applied to the polished surface of the maxillary denture, and the patient was instructed to swallow several times. A check with PIP was then conducted again in order to confirm contact between the tongue and the polished surface of the maxillary denture when the patient swallowed (Fig. 4-2).

Next, impression wax (Adaptol, Jelenko, USA) was used to do the former movement. The patient was asked to phonate several specific sounds. Anterior dental-alveolar sounds (that is, "T" and "D") and palatal-lingual sounds (that is, "Ger" and "Ker") were phonated by the patient alternately. These movements were repeated several times and then checked with PIP (Figs. 4-3, 4-4). The maxillary denture was then processed again for the modified palatal area.

Fig. 5-1: Occlusal view

Fig. 5-2: Lateral view

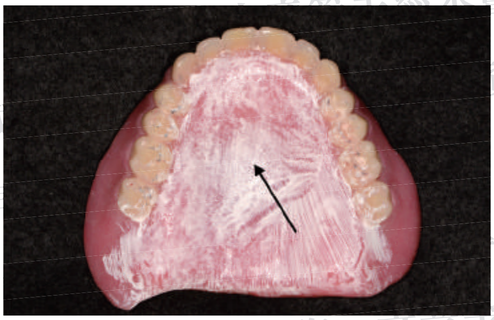

Fig. 5-3: Contact of swallowing

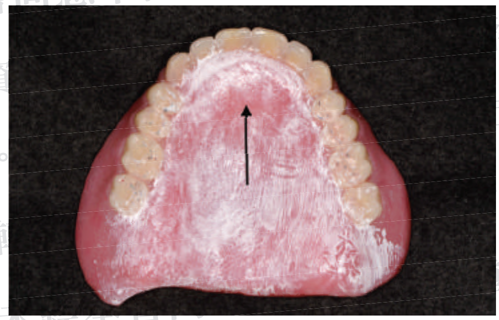

Fig. 5-4: Phonations of "T," "D," and "La"

Fig. 5: Definitive maxillary denture after palatal augmentation

Fig. 6: Intraoral view of dentures

The dentures were prepared for delivery (Figs. 5-1, 5-2). The inspection of the tissue surface and border extension were conducted first; the contact between the tongue and the palatal polished surface of the maxillary denture was checked thereafter (Figs. 5-3, 5-4). Balanced occlusion was achieved and the dentures were delivered to the patient (Fig. 6). The patient was instructed to remove the dentures at night and clean them after meals and before sleeping.

A one-day follow-up visit was arranged with the patient; inspection at that time indicated that his adaptation to the dentures and PAP was acceptable. A small ulcer was noted, however, over the lower left lingual ridge, and the lingual flange of the mandibular denture was adjusted.

After several appointments for adjustment, an examination at the two-year follow-up visit showed that the patient's adaptation was good and his chewing function was substantially improved (Fig. 7).

Fig. 7: Extraoral view of patient (at 2-year follow-up visit)

Discussion

In Taiwan, 95% of oral cancers consist of oral SCC; betel nut chewing and cigarette smoking are the major causes of such SCC and there is a high risk group of 2.5 million people in Taiwan with these habits[6]. Cases of tongue cancer account for about 25-30% of all cases of oropharyngeal cancer[7]. Ablative surgery such as glossectomy is a standard treatment option for tongue cancer patients; however, such forms of surgery always compromise these patients' quality of life.

Previous studies have shown that PAPs can improve the function of the tongue during food consumption[3]. There are, however, some aspects of PAP use that are of concern in patients who have undergone a tongue surgery. Aspiration frequently occurs in patients who have undergone glossectomy, and this complication needs to be reduced or eliminated due to the high risk of death it entails. In a previous study by Davis[8], the patient was reported to have had 20% aspiration initially but then no aspiration after PAPs were inserted.

Articulation is also another issue, because unclear pronunciation is always distressing for patients. In related previous studies, the speech measurements of patients given PAPs were evaluated. Robbins et al.[9] evaluated 10 patients who received PAPs after glossectomy to reduce the space between the palate and tongue to permit better oral deglutition. Voice recordings of these patients were made and evaluated on a scaled score ranging from 0 to 10 points. The average long-term improvement of the patients' articulation scores was 2.2 points.

Several studies have evaluated oral and pharyngeal transit times. In normal people, both times are approximately one second. In Marunick's review study[5], with PAPs inserted, the oral transit time was improved in 11 of 12 subjects, while 6 of 9 subjects had decreased pharyngeal transit time. However, the texture and consistency of the food specimens used in those studies were not reported.

A 2008 study by Okayama et al.[10] revealed that wearing PAPs can reduce not only the duration of contact with the palate but also the total duration of lingual movement. The mean durations of lingual-palatal contact and lingual movement in patients without PAPs were 805.4 ± 306.0 ms and 1612.2 ± 478.3 ms, respectively; in those with PAPs, the times were 621.8 ± 364.9 ms and 1245.6 ± 272.5 ms, respectively. Both times thus showed statistically significant decreases in those with PAPs ($P=0.03$).

The clinical procedures of this report have discussed the fabrication method utilized in making a PAP. Most of the steps used were similar to those used to make conventional complete dentures. The difference was in the application of impression materials to the polished surface of the maxillary denture. Without dentures, the edentulous patient could swallow smoothly due to the lack of vertical dimension and because the tongue could touch the palatal side easily. When the dentures were inserted, the vertical dimension was increased and the patient could not perform the former movement well due to impaired tongue movement. The impression compound was thus used at the beginning to create a lower level palate. And when the patient phonated, the teeth of the opposing arch separated, resulting in an increased vertical dimension. Therefore, the contact between the tongue and the palatal polished surface of the maxillary denture became uncertain. Hence, impression wax was used to mold the movement of phonation. A final check was then done with PIP to confirm actual contact between the tongue and the palatal polished surface of the maxillary denture.

Patients following glossectomy are compromised with prosthetic therapies. Surgical treatment involving the oral cavity often changes anatomical features, resulting in effects such as impaired function of the tongue, compromised condition of the alveolar ridge, reduced load-bearing area, and the reduction of salivary secretions. Therefore, it may be very difficult to restore the oral functions to their presurgical levels. The use of dental implants for such patients may offer some advantages, such as improving the stability and retention of prostheses[11].

Although the patient described in this report could not afford implant placement, his adaptation to dentures was still acceptable. A patient's ability to adapt to new dentures is of substantial importance, as are the methods used for denture fabrication. Patient satisfaction with dentures is associated with age, the number of previous dentures, level of education, period of edentulousness, and self-perceptions regarding one's life[12]. The denture bearing area is also another key factor.

The occlusal scheme in this case was arranged to achieve balanced occlusion with denture stability. The maxillary denture was thicker than a normal complete denture, but the retention was acceptable, perhaps due to a sufficient weight-bearing area. If the increased thickness of a denture is excessive, hollowing out of the denture might be considered to decrease the weight of the denture.

The use of PAPs can have positive effects for patients who have undergone a glossectomy. The acceptable final results seen in this case may be attributed to the obedience to a step-by-step treatment protocol and high patient tolerance.

References

1. Cantor R, Curtis Ta, Shipp T, Beumer J 3rd, Vogel BS. Maxillary speech prostheses for mandibular surgical defects. J Prosthet Dent 1969;22:253-60.
2. Jaradeh S. Neurophysiology of swallowing in the aged. Dysphagia. 1994;9:218-20.
3. Mark M, Nicholas T. The efficacy of palatal augmentation prostheses for speech and swallowing in patients undergoing glossectomy: A review of the literature. J Prosthet Dent 2004;91:67-74.
4. Zarek A. Psychological responses of patients after partial or total glossectomy due to carcinoma of the oral cavity. Ann Acad Med Stetin 2006;52 Suppl 3:113-7.
5. Beumer J, III, Curtis TA, Marunick MT. Maxillofacial rehabilitation. Prosthodontic and surgical considerations. 1996; pp113-223.
6. Kao SY, Lim E. An overview of detection and screening of oral cancer in Taiwan. Chin J Dent Res 2015;18(1):7-12.
7. Ho PS, Ko YC, Yang YS, Shieh TY, Tsai CC. The incidence of oropharyngeal cancer in Taiwan: an endemic betel quid chewing area. Oral Pathol Med 2002:31:213-9.
8. Davis JW, Lazarus C, Logemann J, Hurst PS. Effect of a maxillary glossectomy prosthesis on articulation and swallowing. J Prosthet Dent 1987;57:715-9.
9. Robbins KT, Bowman JB, Jacob RF. Postglossectomy deglutitory and articulatory rehabilitation with palatal augmentation prostheses. Arch Otolaryngol Head Neck Surg 1987;113:1214-8.
10. Okayama H, Tamura F, Kikutani T, Kayanaka H, Katagiri H, Nishiwaki K. Effects of a palatal augmentation prosthesis on lingual function in postoperative patients with oral cancer: coronal section analysis by ultrasonography. Odontology 2008; 96:26-31.
11. Schoen PJ, Reintsema H, Raghoebar GM, Vissink A, Roodenburg JL. The use of implant retained mandibular prostheses in the oral rehabilitation of head and neck cancer patients. A review and rationale for treatment planning. Oral Oncol. 2004; 40(9):862-71.
12. Celebi A, Knezovi -Zlatari D, Papi M, Carek V, Bauci I, Stipeti J. Factors related to patient satisfaction with complete denture therapy. J Gerontol A Biol Sci Med Sci. 2003 ;58(10):948-53.

Case Report

Reversal of the Intrusion of a Natural Tooth between Two Adjacent Implant Restorations: A Clinical Case Report

Chia-Hsien Wang, DDS
Resident Doctor, Department of Prosthodontic Dentistry, Taipei Medical University Hospital, Taipei, Taiwan

May-Show Chen, DDS, MS
Attending Doctor, Department of Prosthodontics, Taipei Medical University Hospital, Taipei, Taiwan
Assistant Professor, School of Dental Hygiene, College of Oral Medicine, Taipei Medical University, Taipei, Taiwan

Bou-Yue Peng, DDS, MS
Attending Doctor, Department of Oral Surgery, Taipei Medical University Hospital, Taipei, Taiwan
Instructor, School of Dentistry, College Of Oral Medicine, Taipei Medical University, Taipei, Taiwan

Shang-Lun Kuo, DDS, MS
Attending Doctor, Department of Prosthodontic Dentistry, Taipei Medical University Hospital
Lecture, School of Dentistry, College of Oral Medicine, Taipei Medical University, Taipei, Taiwan

Hsiu-Na Lin, DDS
Attending Doctor, Department of Prosthodontics, Taipei Chang-Gung Memorial Hospital, Taipei, Taiwan

Chien-Chih Chen, DDS, MS, PhD
Attending Doctor, Department of Prosthodontics, Cardinal Tien Hospital, Taipei, Taiwan

Demeral David Liu, DDS, PhD
Attending Doctor, Department of Periodontology, China Medical University Hospital,
Professor, School of Dentistry, College of Oral Medicine, China Medical University, Taichung, Taiwan

Corresponding author:

May-Show Chen, DDS, MS
Attending Doctor, Department of Prosthodontic Dentistry, Taipei Medical University Hospital
Lecture, School of Dentistry, College of Oral Medicine, Taipei Medical University, Taipei, Taiwan
No. 252, Wuxing St., Xinyi Dist., Taipei City 11031, Taiwan R.O.C.
Tel: +886-2-2737-2181#3211#5
E-mail: mayshowc@hotmail.com

Abstract

Conventionally, the intrusion of an abutment tooth in tooth-implant-supported fixed partial dentures is a troublesome problem, especially in dentures with non-rigid connectors. The clinicians have previously reported that the intrusion of a natural tooth also can be induced when the natural tooth is bounded on both sides by an implant restoration. This unusual case report discusses the case of a 58-year-old female who suffered from infra-occlusion of the upper left first premolar following the sequential implantation of restorations over the adjacent canine and second premolar. In addition to the infra-occlusion, a 6 mm pocket and an angular bony defect on the mesial side of this tooth associated with a PDL widening, tight proximal contacts, and a mild percussion pain were noticed. In order to resolve the infra-occlusion, the old PFM restoration was removed and restored with a provisional crown with open interproximal and occlusal contacts. After one year of intensive and sequential adjustments of the proximal and occlusal contacts, the intrusion of the upper left first premolar was almost completely reversed and the periodontal defect was significantly improved.

Key words: dental implant, implant prostheses, tooth intrusion

Introduction

Conventionally, the intrusion of an abutment tooth in tooth-implant-supported fixed partial dentures is a troublesome complication, especially in dentures with non-rigid connectors[1, 2, 3]. Several theories have been proposed to address this issue, but the mechanisms underlying the responses to this intrusion phenomenon remain unclear[4, 5, 6, 7]. In addition to such conventional intrusion of a natural abutment in a tooth-implant-supported fixed prosthesis, the clinicians have previously reported the intrusion of a free-standing natural tooth when the natural tooth is bounded on both sides by an implant restoration[8].

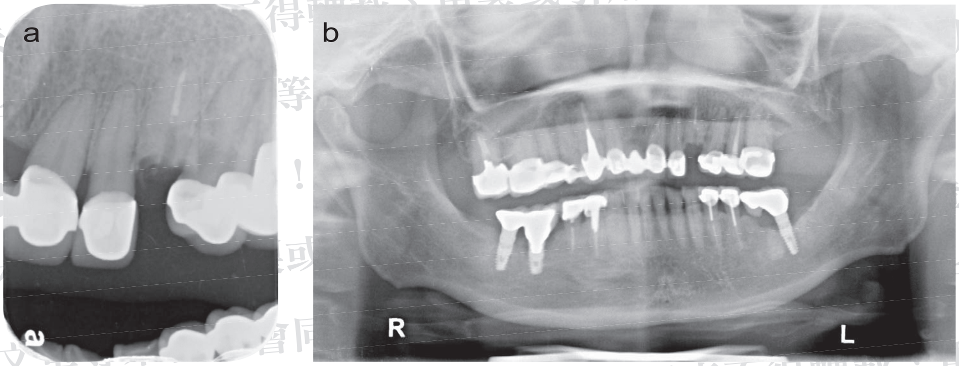

Fig. 1 Periapical and panoramic radiographs of tooth #23, an unrestorable fractured tooth, which was extracted in the following treatment sequence.

Fig. 2 Periapical radiograph of tooth #23, which was replaced with an implant-supported prosthesis on July 9, 2013.

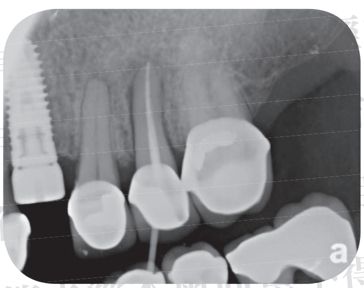

Fig. 3 Periapical radiograph of tooth #25, an unrestorable fractured tooth, which was extracted in the following treatment sequence.

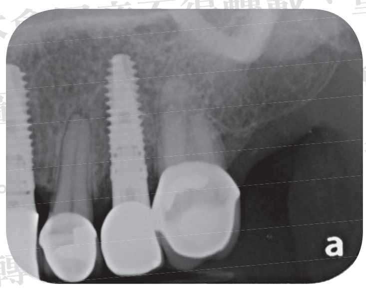

Fig. 4 Periapical radiograph of tooth #25, which was replaced with an implant-supported prosthesis on June 11, 2014.

Fig. 5 Tooth #24 was shown to exhibit infra-occlusion in a clinical examination.

In this unique case report, we sought to describe this unusual intrusion phenomenon of a natural tooth intruding right between two adjacent implant restorations and to provide a solution for reversing the intrusion and fixing the associated periodontal defects.

Clinical Report

A 58-year-old partially dentate woman came to the Department of Prosthodontics of Taipei Medical University Hospital for the restoration of a fractured upper left canine on November 26, 2012.

In the intra-oral and radiographic examination, we found that tooth #23 (according to the FDI system of tooth nomenclature) was fractured and not restorable (Fig. 1). Therefore, tooth #23 was extracted and replaced on December 11, 2012, with a dental implant (Xive®; FRIADENT) 4.5 mm in diameter and 13 mm in length, following the standard protocol. The dental implant in the tooth #23 area was uncovered and loaded uneventfully six months later on July 9, 2013, with a cement-retained all-ceramic crown restoration (Fig. 2). At the impression appointment for the dental implant restoration of the tooth #23 area, a fistula with a solitary deep narrow pocket was found over the buccal side of tooth #25, and a root fracture was suspected (Fig. 3). So, tooth #25 was extracted and replaced on November 14, 2013, with a dental implant (Xive®; FRIADENT) 3.8 mm in diameter and 13 mm in length. The dental implant in the tooth #25 area was restored with a cement-retained zirconia crown on June 11, 2014 (Fig. 4).

During a routine check-up conducted on September 11, 2015, the patient complained that tooth #24 between the two dental implant restorations had become shorter with an unpleasant progressive enlargement of the inter-occlusal gap (Fig. 5). Upon conducting an intra-oral examination, we found infra-occlusion of tooth #24 with a tight proximal

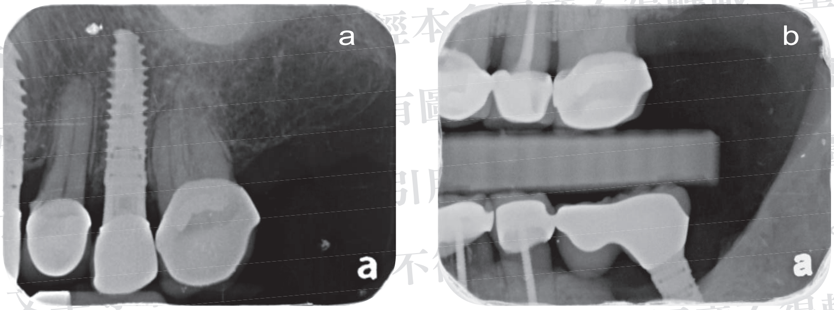

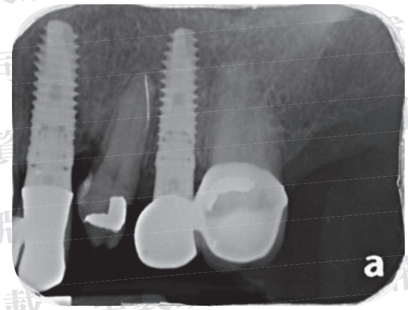

Fig. 6 (a) Periapical radiograph before crown removal of tooth #24 on September 23, 2015.
(b) Bitewing radiograph showing the gap beneath the original crown tooth #24 in 2012.

Fig. 7 Periapical radiograph after crown removal of tooth #24 on September 23, 2015.

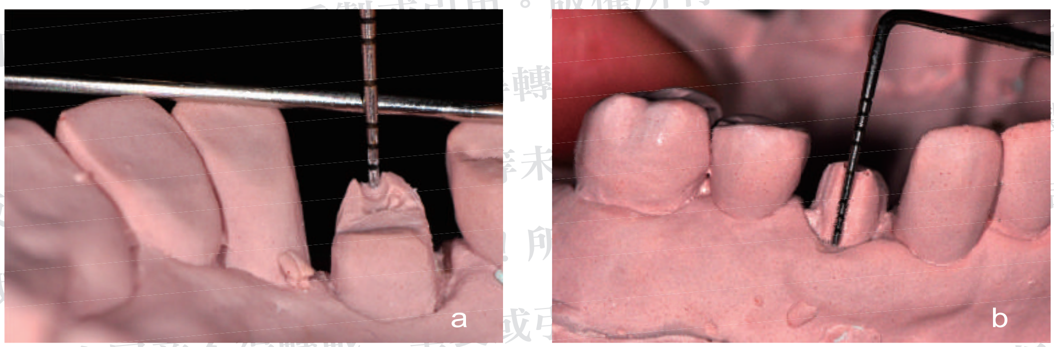

Fig. 8 Stone cast of the relationship between tooth #24 and the tooth #25 dental implant made on September 23, 2015.

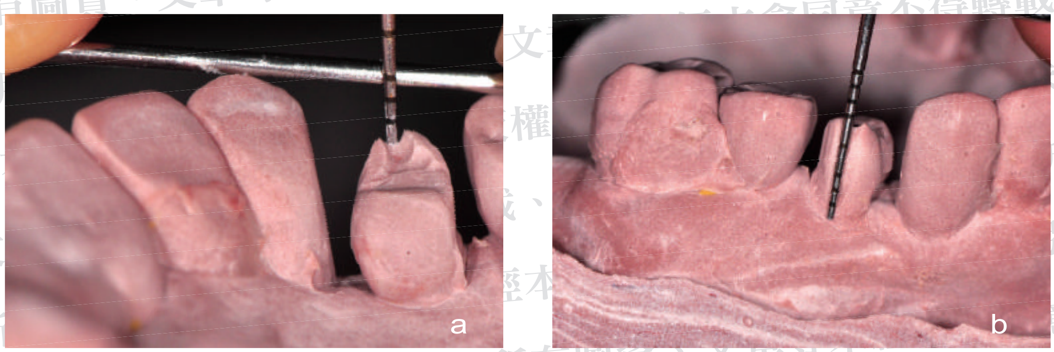

Fig. 9 Stone cast of the relationship between tooth #24 and the tooth #25 dental implant made on September 27, 2016.

contact and a 6 mm mesial pocket depth. A periapical radiograph revealed that the root apex of tooth #24 was at the level of the 5 screw thread from the apex of the tooth #25 dental implant, and an angular bony defect was found on the mesial side of tooth #24 (Fig. 6). However, the root apex of tooth #24 had been at the level of the 7 screw thread from the apex of the tooth #25 dental implant at the time of the insertion of the implant-supported prosthesis (Fig. 4). Tooth #24 showed grade I mobility and mild percussion pain (Fig. 6). To solve the infra-occlusion problem and address the associated clinical symptoms and signs, and to fix the gap between the tooth structure and the porcelain-fused-to-metal crown of tooth #24 (Fig. 6-b), the crown was removed and the provisional crown was delivered without occlusal and proximal contacts (Fig. 7). Because we intentionally reversed the intrusion, biting sensitivity, and periodontal defects, the patient was put on an intensively regular one-month follow-up schedule. Scaling/root planning, local subgingival curettage, and oral hygiene instruction were

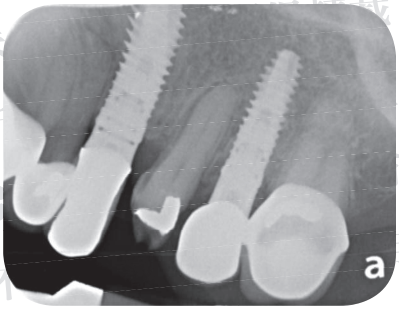

Fig. 10 Periapical radiograph of the relationship between tooth #24 and the tooth #25 dental implant on September 27, 2016.

performed. In addition to the periodontal care, the adjustment of the provisional crown was performed to remove occlusal and proximal contacts. One year after the delivery of the provisional crown, tooth #24 had been extruded by 2.5 mm (Figs. 8, 9), and the periodontal condition was significantly improved while the percussion pain was substantially relieved. More importantly, the periodontal reevaluation data regarding tooth #24 showed a decrease in the mesial probing depth and the tooth's mobility. In addition to this clinical improvement, periapical radiography revealed that the root apex of tooth #24 was at the level of the 6.5 screw thread from the apex of the tooth #25 dental implant, with a significant reduction of the mesial angular bony defect and improvement of the trabecular projection (Fig. 10).

Discussion

Various biological and mechanical complications of dental implants have been reported in the previous literature. The intrusion of an abutment tooth in tooth-implant-connected fixed partial dentures is one common problem affecting such dentures. Various possible reasons for the intrusion of an abutment tooth have been proposed, including: (1) disuse atrophy, (2) differential energy dissipation, (3) mandibular flexure and torsion, (4) flexure of fixed partial denture frameworks, (5) impaired rebound memory, (6) debris impaction or microjamming, and (7) the ratchet effect[4-7, 9-12]. To the best of our knowledge, only one clinical report in the previous literature has discussed the intrusion of a free-standing natural tooth adjacent to implant restorations[8]. In that article, Wang et al.[8] suggested that the possible mechanisms underlying the response to such an intrusion are the impaired rebound memory and mechanical binding. Furthermore, the uneven marginal ridges described in their case might have contributed to the intrusion and mechanical locking between the contact areas of the two adjacent osseointegrated implant-supported prostheses. The impaired rebound memory and mechanical binding were proposed for the further intrusion. In our clinical scenario, the intrusion of the upper left first premolar tooth did not occur when only one adjacent implant restoration, for the upper left canine, was placed. This might have been due to the resilience of the periodontal ligament of the upper left distal second premolar providing movement and rebound of this natural tooth.

Once both adjacent implant restorations had been delivered, however, the intrusion of this natural tooth was prominent. In the aforementioned previous report, Wang et al.[8] only removed the distal proximal contact to allow the spacing for reversal of the intrusion. However, we reduced the occlusal and both proximal contacts to allow for extrusion of the intruding tooth due to the future replacement of its old PFM crown. The article by Wang et al.[8], which was based on their clinical observations, suggested two clinical guidelines. First, when a natural tooth is bounded by implant restorations on both sides, the contact area should be carefully adjusted to prevent intrusion of the natural tooth. Second, reversal of an intrusion of this type may occur if the contact areas are corrected. In the current case, we intentionally aimed to free the occlusal and proximal contacts to reverse the periodontal defects and infra-occlusion induced by a natural tooth bounded on both sides by two sequential dental implants.

This clinical case report describes the treatment and management of the intrusion of a natural tooth bounded by two adjacent implant restorations. Though the mechanisms underlying the response to such an intrusion remain unclear, the reversal of the intrusion and periodontal defects were obtained after an intensive series of adjustments of the proximal and occlusal contacts.

References

1. Wei H, Tomotake Y, Nagao K, Ichikawa T. Implant prostheses and adjacent tooth migration: preliminary retrospective survey using 3-dimensional occlusal analysis. Int J Prosthodont 2008; 21:302-4.
2. Daftary F, Mahallati R, Bahat O, Sullivan RM. Lifelong craniofacial growth and the implications for osseointegrated implants. Int J Oral Maxillofac Implants 2013; 28:163-9.
3. Pikner SS, Gröndahl K, Jemt T, Friberg B. Marginal bone loss at implants: a retro- spective, long-term follow-up of turned Branemark System implants. Clin Implant Dent Relat Res 2009; 11:11-23.
4. English CE. Root intrusion in tooth-implant combination cases. Implant Dent 1993;2:79-85.
5. Sheets CG, Earthman. Natural tooth intrusion and reversal in implant-assisted prosthesis: Evidence of and a hypothesis

for the occurrence. J Prosthet Dent 1993; 70:513-20.

6. Shrets CG, Eathinan JC. Tooth intrusion in implant-assisted prosthesis. J Prosthet Dent 1997; 77:39-45.
7. Pesun IJ. Intrusion of teeth in the combination implant-to-natural-tooth fixed partial denture: A review of the theories. J Prosthodont 1997; 6:268-77.
8. Tong-Mei Wang, Ming-Shu Lee, Sang-Heng Kok, Li-Deh Lin. Intrusion and reversal of a free-standing natural tooth bounded by two implant-supported prostheses: A clinical report. J Prosthet Dent 2004; 92:418-22.
9. Rieder CE, Parel SM. A survey of natural tooth abutment intrusion with implant-connected fixed partial dentures. Int J Periodont Rest Dent 1993; 13:335-47.
10. Cho GC, Chee WW. Apparent intrusion of natural teeth under an implant supported prosthesis: A clinical report. J Prosthet Dent 1992; 68:3-5.
11. Strflik DE, Parr GR, Sisk AL. Histomorphometry of the dental implant-bone interface: One year result of a comparative investigation in dogs. Int J Oral Maxillofac Implants 1994; 9:501-12.
12. Steflik DE, Sisk AL, Parr G. Correlative transmission electron microscopic and scanning electron microscopic observation of the tissues supporting endosteal blade implants. J Oral Implants 1992; 18:110-20.

Instructions for authors

The Journal of Prosthodontics and Implantology is an official publication of the Academy of Prosthetic Dentistry, ROC, published quarterly in April, July, November and January. Articles related to clinical and basic prosthodontics, implantology, implant related periodontology, periodontology and surgery as well as biological and material sciences related to prosthodontics and implantology are welcome. Articles may be categorized as original paper, case report, technical reports and literature review related to future research. Invited review articles are written by representative scholars on some important topics this journal wishes to emphasize.

Submitted papers will be evaluated by the editorial board and invited reviewers. Papers submitted shall not be accepted or published by any other journals. Papers published in this journal will become the copyright of this journal and shall not be subsequently published in any other publication in any language without prior written consent of the publisher.

Manuscript should be prepared according to the guidelines produced by the International Committee of Medical Journal Editors: Uniform Requirements for Manuscripts submitted to Biomedical Jopurnals. Further information can be found at http://www.icmje.org.

Manuscript should be submitted via e-mail at the address of: prosthor@ms48.hinet.net

The manuscript format

1. Title page: including title, names and institutions of each author. Corresponding author should also provide mailing address, phone and fax number and e-mail address. A running title no more than 40 words and no more than 4 keywords should also be provided.
2. Abstract: no more than 400 words, should briefly describe the purposes of the study, material and methods used, results and discussion with conclusion.
3. Text:
   A. Review articles: can be of author's preferred format.
   B. Original articles: should include introduction, materials and methods, results, discussion and conclusion.
   C. Case reports and technical reports: should include introduction, case or technique description and discussion.
4. References: All publications cited in the text should be presented in the references part. The order of references should follow the order cited in the text. Examples of the reference style of this journal are as follow:
   A. Journal reference style: List all authors if the number is six or less. If author number is more than six, list six authors and add et al for the remaining authors.
      (1) Journal article: Lin YT, Chang LC. Space changes after premature loss of the mandibular primary first molar: a longitudinal study. J Clin Pediatr Dent 1998; 22: 311-6.
      (2) Online journal article: Yavuz MS, Aras MH, Büyükkurt MC, Tozoglu S. Impacted mandibular canines. J Contemp Dent Pract 2007; 8: 78-85. Available at: http://www.thejedp.com/issue036/index.htm. Accessed November 20, 2007.
   B. Book reference style:
      (1) Complete book: McDonald RE, Avery DR. Dentistry for child and adolescent. 5th ed, Mosby Co, St Louis, 1988; pp339-41.
      (2) Chapter in book: Moore BK, Avery DR. Dental materials. In: McDonald RE, Avery DR (ed). Dentistry for child and adolescent. 6th ed., Mosby Co., St. Louis, 1994; pp349-72.
5. Tables and figures: should be kept in minimum number. Figures should be in JPG, EPS or TIF file and can be e-mailed to the editor. They should be clear enough and listed in separated pages. Scale marker should be provided for magnification. All abbreviations shown on the table and figure should be explained in the legend.

   Photos of patients should be obscured for identification. Otherwise a patient's consent form should be provided.

投 稿 須 知

一、 本期刊為季刊，每年四、七、十及一月出刊，以英文刊出。

二、 凡與基礎或臨床補綴學、顳顎關節或咀嚼功能、人工植體相關、牙科補綴之技工學有關之著作，均為刊載之對象。接受的稿件類型共有下列五種，來稿請註明類型：

1. 社論(editorial)
2. 學術綜論(review article，限邀稿)
3. 研究論文(original artic1e)
4. 病例報告(case report)
5. 技術報告(technical report)

三、 稿件撰寫一般格式:

1. 稿件必須是沒有刊出或將被接受刊於其他雜誌者。
2. 以英文投稿，文章內容以複行 (double spacing) 繕打，字體大小12以上，其每邊邊緣至少須留2.5公分，不須任何格式編排。
3. 全文總頁數 (包括摘要、圖、表、參考文獻) 以八頁為限，必要時可增至十二頁。
4. 請以電子文件投稿，文書處理程式建議以IBM-Microsoft Word為主。須標示使用程式、投稿題目、第一作者姓名，將電子文件e-mail至: prosthor@ms48.hinet.net。
5. 請同時附上致本誌主編簡短信函，表明投稿本誌之意願，並說明所有著者均曾過目並簽名同意。若為人體試驗須附人體試驗委員會之同意函。

四、 稿件內容詳細規格如下:

1. 首頁 (title page)：包括題目、作者姓名、服務單位、學歷；英文簡題(running title)長度在四十個字以內；稿件主要負責者(corresponding author)之英文姓名與地址、電話、傳真、e-mail。
2. 摘要 (abstract)：以400字為限，簡潔說明並標示研究目的、方法、結果、主要結論或新發現。若為原始著作則須說明並標示，並需附關鍵詞(key words) 5個以內。
3. 本文 (text)：
   A. 學術綜論(review article)—無一定格式。
   B. 原始著作(original article)—分前言、材料與方法、結果、討論、結論。
      (1) 前言 (introduction)：簡要說明研究由來。
      (2) 材料與方法 (material and methods)：敘述研究設計、對象、步驟。
      (3) 結果 (results)：研究結果以文字、表格或插圖表示之。
      (4) 討論 (discussion)：強調重要結果與論點，與前人論述作比較等。
      (5) 結論 (conclusion)：結論要簡要明確。
   C. 技術報告(technical report)—分前言、方法描述、討論。
   D. 病例報告(case report)—分前言、病例描述、討論。

4. 參考文獻 (references)：以出現於本文中之先後順序用阿拉伯數字(上標)排列之，書寫方式請參考Cumulated Index Medicus，內容含作者姓名(全部列出)、篇名、期刊名、年代、頁數。例如：(1)期刊之書寫：Lin YT, Chang LC. Space changes after premature loss of the mandibular primary first molar: a longitudinal study. J Clin Pediatr Dent 1998; 22: 311-6. (2)書籍之書寫：McDonald RE, Avery DR. Dentistry for child and adolescent. 6th ed., Mosby Co, St Louis, 1994; pp339-41. (3)有編輯者之書籍章節書寫：Moore BK, Avery DR. Dental materials. In: McDonald RE, Avery DR. Dentistry for child and adolescent. 6th ed., Mosby Co., St. Louis, 1994; pp349-72. (4)電子期刊之書寫：Yavuz MS, Aras MH, üyükkurt MC, Tozoglu S. Impacted mandibular canines. J Contemp Dent Pract 2007; 8:78-85. Available at: http://www.thejedp.com/issue036/index.htm. Accessed November 20, 2007.

5. 插圖與表格 (figures and tables)：
   (1) 插圖請勿放置於本文中，圖與表之數量盡量少，也不要編排，應儲存於另外的檔案夾。影像圖檔應以JPG、EPS或TIF 形式存檔。插圖以電子檔e-mail傳送投稿。
   (2) 插圖之標題及詳細說明，須另頁複行繕打。顯微照像須以比例尺(internal scale marker)標明放大倍數。
   (3) 病人臉部照片須遮蓋眼睛至無法辨認是何人的程度，否則須附病人之書面同意書。
   (4) 繪圖軟體應使用如Photoshop、Photoimpact、Illustrator等。彩色或灰階圖形須掃瞄至300 DPI，線條圖形則須至1200 DPI，並請標明圖檔名稱及所使用軟硬體名稱。
   (5) 圖或表中出現之字母或符號，均需於註解中詳細解釋。

五、 投稿清單

(1) 致主編簡短信函。
(2) 提供稿件主要負責者之姓名與地址(英文)、電話、傳真、e-mail、所有作者之服務機構(英文)。
(3) 附英文摘要(400字以內)，研究論文的摘要應分研究目的、方法、結果、主要結論。
(4) 附英文關鍵詞(5個以內)；附英文簡題(長度在40個字以內)。
(5) 確認所有參考文獻的格式、內容、引用順序皆完整無誤。
(6) 確認所有表格(標題、註腳)及插圖之標題及詳細說明，另紙複行繕打。
(7) 確認所有圖表皆符合格式。圖表皆儲存於另外的檔案夾，而未放置於本文中。
(8) 若為人體試驗須附人體試驗委員會之同意函。
(9) 全部作者同意簽名之證明函。

六、 稿件一經刊載，版權屬本誌所有；本誌將免費印贈第一作者抽印本20份。

TABLE OF CONTENTS

ISSN 2304-541-8

9 772304 541008